INVESTIGATING STANDARDIZED 3D INPUT DATA FOR SOLAR PHOTOVOLTAIC POTENTIALS IN THE NETHERLANDS

ARSHA YUDITHA AMIRANTI
June, 2020

SUPERVISORS:
dr. M.N. Koeva
dr. M. Kuffer

EXTERNAL SUPERVISORS:
Vincent van Altena (Kadaster)
Marc Post (Kadaster)

INVESTIGATING STANDARDIZED 3D INPUT DATA FOR SOLAR PHOTOVOLTAIC POTENTIALS IN THE NETHERLANDS

ARSHA YUDITHA AMIRANTI
Enschede, The Netherlands, June, 2020

Thesis submitted to the Faculty of Geo-Information Science and Earth Observation of the University of Twente in partial fulfilment of the requirements for the degree of Master of Science in Geo-information Science and Earth Observation.
Specialization: Geoinformatics

SUPERVISORS:
dr. M.N. Koeva
dr. M. Kuffer

EXTERNAL SUPERVISORS:
Vincent van Altena (Kadaster)
Marc Post (Kadaster)

THESIS ASSESSMENT BOARD:
Prof. dr. R. V. Sliuzas (Chair)
Dr.Ir. S.J. Oude Elberink (External Examiner, University of Twente)

ABSTRACT

Nowadays, the usage of 3D models extends beyond visualization purposes, serving as a representation to analyze the real world. Kadaster (the Dutch Land Registry and Mapping Agency) is interested in utilizing 3D models for different applications. This study aimed to explore the possibility to integrate two different point clouds to produce a unified dataset as the input data for 3D model generation that can suit many applications. The suitability of this dataset is tested on a use case of estimating solar photovoltaic analysis.

This study used a mixed qualitative-quantitative method to gather and process the data. In this research, we used the LiDAR point cloud and point cloud derived from a dense image matching (DIM) technique. To gauge the perspectives of the users, we conducted semi-structured interviews and a focus group discussion. Our study found that the main problem when performing data integration is to correctly and accurately integrate the datasets when those datasets have different accuracy, density, and properties. The foundation to determine the quality of the 3D model is to assess the quality of the input data. Following three out of the six elements of data quality from ISO 19157: 2013 (ISO, 2013), we used completeness, temporal quality, and positional accuracy to determine the quality of the input data. These elements were used because those elements have a significant impact on the geometric aspect of 3D data.

We integrated the LiDAR point cloud and the DIM point cloud using the Iterative Closest Point (ICP) algorithm. The major advantage of integrating these two point cloud datasets is to improve the temporal quality, completeness, and positional accuracy. During the semi-structured interview, these three factors were identified as the inadequacy of the quality of the currently used input data. We generated 3D models of 48 buildings semi-automatically using the integrated point cloud, building footprints and manually extracted rooflines using the RANSAC algorithm. The integrated point cloud and the 3D models were both converted into a digital surface model (DSM) as input data for solar photovoltaic potential. Several criteria were applied to determine the potential areas for solar photovoltaic installation that were identified during the semi-structured interview: roof slope, roof orientation and minimum threshold for solar irradiation. To assess the benefit of using the 3D model as input data for solar photovoltaic analysis, we compared the result from the two input data models.

From the result of the experiment, the calculation results of the solar photovoltaic potential are different between the input data models. When using the converted 3D models as input data, the roof details are generalized and noise is removed. The details and noise remained when using the integrated point cloud DSM as input data for the analysis. According to the result of the group discussion, using a 3D model as input data for the solar photovoltaic potential analysis could avoid noise and data gaps. The discussion revealed a hidden benefit and perception from users when using the 3D model, that people prefer to view a representation of reality which 3D can provide for them. Therefore, these findings provide a new understanding that the solar photovoltaic analysis benefits from using the 3D model as the input data and as the visualization for the output.

Keywords: point cloud, LiDAR, dense image matching, 3D model, solar photovoltaic, ICP algorithm, RANSAC algorithm.

ACKNOWLEDGEMENTS

I would like to express my gratitude to my supervisors Dr. Mila Koeva, Dr. Monika Kuffer. Thank you for your patient and constructive guidance, also for giving me the opportunity to undertake this collaborative research with Kadaster. Your enthusiasm encouraged me a lot taught me to think critically and to stay positive.

Thanks to Kadaster for providing me with invaluable knowledge during the whole trajectory of this research. Vincent van Altena, Marc Post, and Bhavya Kausika, thank you for guiding me during the internship also responded to my questions promptly and giving me feedback.

I would like to thank my partner for his continued support and encouragement, who experienced the ups and downs of my research. Thank you for your willingness to proofread countless pages of this research-ik hou van jou. To my family and friends in Indonesia and The Netherlands, thank you for your enormous love, it keeps me going-I love you.

TABLE OF CONTENTS

LIST OF FIGURES

LIST OF TABLES

1. INTRODUCTION

Variations of input data can cause serious problems, which, for example, is illustrated by the differing results of environmental impact assessment (milieueffectrapport (MER)) from 2013 on Lelystad Airport in The Netherlands. Analysis has discovered that it contains errors in assessing noise pollution ("Fouten bij berekening geluid Lelystad," 2017; van de Bor, 2019). The main problem was the input data, and the height profile used did not meet the requirements for noise calculation, which lead to the wrong results.

Therefore there is a need to investigate a standard of input data to have a consistent and reliable result. With the increase of technical development, GIS technology and 3D dataset (height representation), are widely utilized for environmental analysis. However, the major challenge lies in the uncertainty of the outcome as a result of the quality and spatial detail of the input data.

This study investigates the influence of different 3D input data for solar photovoltaic potential analysis and taking user requirements into account. This section consists of background and justification with supporting literature, research gap, problem, objectives and research questions.

1.1. Background and justification

Nowadays, the usage of 3D models is extended beyond visualization purposes. Incorporated with the application of GIS, it gains insights into the richer spatial analysis. Therefore, city authorities and national mapping agencies such as Kadaster (the Dutch Land Registry and Mapping Agency) are interested in utilizing 3D models for different applications.

Several studies have assessed the utilization of 3D models (see Biljecki, Stoter, Ledoux, Zlatanova, & Çöltekin, (2015)). However, because of the differences in the input data, the results differ in quality even when they are being applied to the same area and were retrieved the same methods (Peters, Commandeur, Dukai, & Stoter, 2018). The differences in the input data make the results incomparable, unreliable, and inefficient. Kadaster, as a geodata provider in The Netherlands, acknowledges this situation, and they are interested to research in which way standardization of 3D input data contributes to alleviate these issues in estimating the solar photovoltaic potential.

1.2. Research problem

Taking part in the global effort to develop an energy economy that is safe, reliable, and affordable, The Netherlands adopted the 'Energy Agreement for Sustainable Growth' in 2013 (Ministry of Economic Affairs of the Netherlands, 2016). In that energy policy, the Dutch cabinet has defined three main targets: (1) prioritize CO2 reduction; (2) optimize economic opportunities of the energy transition; (3) include energy transition targets into spatial planning policy. In general, solar energy considered to be one of the key renewable energy sources to achieve these transition targets (Paardekooper, 2015). Therefore simulations or prediction analysis are important approaches to stimulate renewable energy transition.

Extensive collections of geodata are available in the Netherlands. These can be modeled for many simulations and prediction analysis. However, modeling input data for that simulations and prediction analysis is crucial. Such data is *Basisregistratie Addressen en Gebouwen* (BAG)[1], *Actueel Hoogtebestand Nederland* (AHN)[2], and point cloud derived from aerial imagery using dense image matching (DIM). Each input geodata has its own characteristics, which makes 3D modeling challenging.

For instance, the quality of both point cloud datasets differs. One of the features to measure the quality of a point cloud expresses the number of points per square meter, which is called point density. Higher density represents high accuracy. The number of points is dependent on the sensor and flying height. Also, the data acquisition techniques are different. AHN is a high-resolution LiDAR point cloud dataset of the Netherlands. The most recent dataset was released in 2019 with a data acquisition period of six years (Actueel Hoogtebestand Nederland, n.d). The advantages of AHN are: (1) publicly available, (2) acquired from LiDAR, and (3) able to penetrate vegetation. The drawbacks are: (1) the data acquisition time intervals (temporal resolution) are large, and (2) the point density is low due to the flying height. These drawbacks of the LiDAR point cloud can be compensated with a DIM point cloud derived from aerial imagery (Altuntas, 2015).

In the Netherlands, aerial imagery is acquired twice a year during summer and winter with aerial photogrammetry (Beeldmateriaal Nederland, n.d.). The advantages of these data are (1) high temporal resolution and (2) higher point density. The drawbacks of these data are (1) it is not publicly available, (2) objects can be obstructed by vegetation. Although both data are in point clouds form, the properties of LiDAR point cloud and point cloud generated from dense image matching are different (Table 1).

Table 1. Techniques for the point cloud generation.

Properties	LiDAR	DIM
Acquisition	From a satellite, airborne, terrestrial and mobile.	From satellite, airborne and terrestrial photogrammetry.
Sensor	Laser.	Camera.
Output	Point clouds	Point clouds from the result of calculation of depth value for each pixel of an image.
Number of return	Multiple returns	N/A

The integration from the above-mentioned techniques are commonly used to reconstruct precise 3D models (Altuntas, 2015; Mwangangi, 2019; Oude Elberink & Vosselman, 2011; Vosselman, 2012; Xiong, Oude Elberink, & Vosselman, 2016). However, the main challenge when performing data integration is to correctly and accurately integrate the datasets when those data sets are characterized by different accuracy, density and properties (Kaartinen et al., 2005; Kedzierski & Fryskowska, 2015; Rottensteiner et al., 2014). The current study aims to explore the possibility to integrate two different point clouds to produce a unified dataset that can suit many applications. The suitability of this dataset will be tested on a use case of estimating solar photovoltaic analysis.

The solar photovoltaic potential is derived from solar radiation calculation. As stated by Machete (2016) and Esri (2007), incoming solar radiation (insolation) that arrives at a surface can be distinguished in direct, diffused and reflected radiation. Direct radiation is the strongest component of the total radiation (Figure 1), described as solar radiation that is traveling from the sun to the earth surface without obstacles. Diffused radiation is the second strongest component, which is described as solar radiation that scatters from the

[1] https://www.pdok.nl/introductie/-/article/basisregistratie-adressen-en-gebouwen-ba-1
[2] https://www.pdok.nl/introductie/-/article/actueel-hoogtebestand-nederland-ahn3-

direct solar beam before reaching the earth surface. Reflected radiation is the least strong radiation that contributes to the total radiation, described as radiation reflected from ground or any urban element.

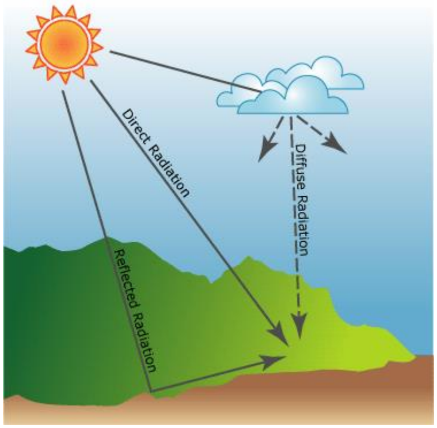

Figure 1. Illustration of different type of solar radiation arrived at the surface. (Source of image: (ESRI, 2007)

For estimating the solar photovoltaic potential, there are two approaches a 2.5D approach and a 3D approach (Freitas, Catita, Redweik, & Brito, 2015). The differences between 2.5D and 3D are explained in Section 2.3.3. These approaches determine the representation of the input data. The 2.5D approach uses a DSM as its input data and is mostly derived from LiDAR data (Peronato, Rey, & Andersen, 2018), while the 3D approach uses a 3D model as its input. According to Peronato et al. (2018) and Machete (2016), the reflected radiation is not taken into account when using 2.5D for roof surfaces calculation. On the other hand, when 3D data is used in calculating the solar radiation, all three components direct, diffuse and reflected radiation can be calculated.

Thus this research aim is to assess the shortcomings of the current input data and its impact on 3D analysis in the application of estimating the solar photovoltaic potential. Moreover, it assesses the influence of pixel resolution and the usage of the 3D model as input data for estimating solar photovoltaic potential.

1.3. Research objectives

1.3.1. General objectives

To develop a standardized 3D input data model for the specific use case of a solar photovoltaic potential analysis.

1.3.2. Sub-objectives

1. To investigate the characteristics of the input data for 3D model.
2. To prepare unified data that satisfy the user needs for 3D model.
3. To develop a 3D model to estimate the potential of a solar photovoltaic installation.

1.3.3. Research questions

Sub-objective 1:

1. What are the current problems of the input data?
2. How to determine the quality of the input data?
3. How to improve the quality of the input data currently used for 3D modeling?

Sub-objective 2:

1. What is the required information to estimate solar photovoltaic potential?

2. What LOD is required for 3D solar photovoltaic analysis?
3. What is the compliance between the user requirements and the existing data?

Sub-objective 3:

1. Which method is suitable to develop the 3D model?
2. Which method is suitable to estimate the potential of solar photovoltaic?
3. Does the developed 3D model improve the accuracy of the estimation of the potential solar photovoltaic?
4. How does the developed model fit the purpose of the application?

1.3.4. Anticipated results

1. Description of a suitable input data model for 3D model.
2. Unified dataset for 3D modelling that is suitable for solar photovoltaic analysis.
3. 3D model for solar photovoltaic analysis.

1.4. Conceptual framework

Figure 2 illustrates the relationship between concepts applied in this research. The 3D input data as the main core of this research is widely available and commonly used as the main input for simulation and prediction analysis for different types of applications. However, the 3D input data is different in the acquisition, temporal and spatial resolution, which makes the characteristics of the data different. We aimed to develop a standardized 3D input data to be used in support of a variety of applications. Each application has its own requirements to produce a reliable output and consistent quality. The quality in 3D data is perceived following the data spatial quality elements. To obtain a sufficient quality for the purpose of the application, we gauged the perceptions of the users and identified the shortcomings of the currently available 3D input data. Therefore this research combines these three concepts, i.e. 3D input data, users' perception and application to achieve a unified 3D input data that is usable for any applications following the users' needs.

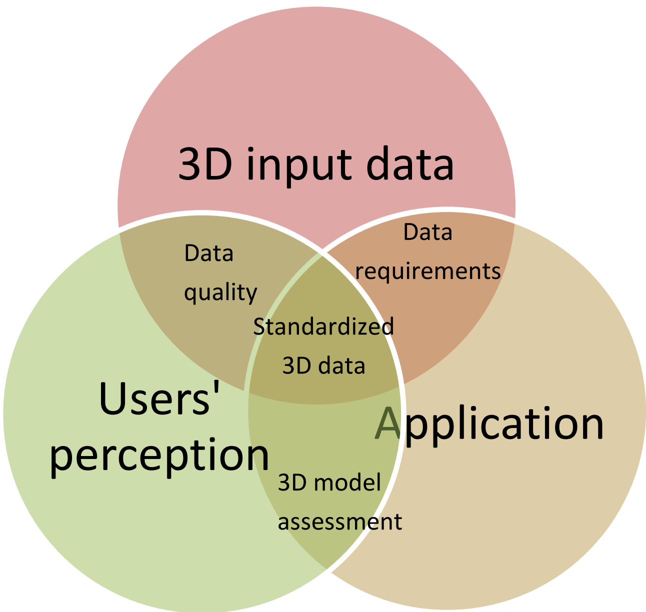

Figure 2. Conceptual framework of this study.

1.5. Thesis structure

This thesis contains five chapters:

Chapter 1, introduction, explains the background and justification of the study; the objectives of the study and its contribution to filling the gap both in academic research and in practice; also research questions.

Chapter 2, the literature review, gives an overview of related previous studies and the current state of the study.

Chapter 3, methodology, explains the used methods in this study. Also, it provides a rationale for study area selection, its current issue and data description.

Chapter 4, results and discussions, present the results and answers to each research questions.

Chapter 5, conclusions and recommendations, provide findings on the role of a standardized 3D model for estimation solar photovoltaic. This chapter presents findings for each answer to the research questions, and suggestions for further research are proposed.

1.6. Summary

Differences in input data for different applications often leads to inconsistent results. Kadaster, in its role as a geodata provider for the Netherlands, is interested in the establishment of a standard 3D data model to produce consistent and comparable results that can be used for different applications. In this research, we test the suitability of the 3D data models on a use case of estimating solar photovoltaic analysis. Major steps in this research are (1) the creation of a unified dataset; (2) generation of 3D model; (3) the identification of the perspectives of the users; and (4) the estimation of solar photovoltaic potential using the 3D model.

2. LITERATURE REVIEW

The objective of this chapter is to describe relevant literature, the state-of-the-art for 3D data and its usage in the solar photovoltaic potential analysis. The chapter starts with the elaboration of 3D data in section 2.1. Section 2.2 discusses data integration. The next section (section 2.3) discusses the role of a 3D model in the application of solar photovoltaic potential analysis and the relation between the 3D model and solar photovoltaic analysis. Section 2.4 provides a summary of this chapter and answer sub-objective 1.

2.1. 3D data

This section describes the acquisition of 3D data (section 2.1.1), the characteristics of 3D data (section 2.1.2), the quality of 3D data (section 2.1.3), and the usage of 3D data for generating 3D models (section 2.1.4).

2.1.1. Acquisition of 3D data

Real-world can be represented using 3D models. These 3D models are created using different data sources (see Biljecki, Ledoux, & Stoter (2016)). Direct acquisition using aerial or terrestrial surveying is the most common approach to collect 3D data from reality. However, direct acquisition is not the only process to collect 3D data from reality. They can also be obtained from digitizing process or architectural design. After capturing process is finished, through the augmentation process that consists of 3D reconstruction and data integration, the 3D model can be generated (Figure 3). This augmented process is presented in several works, photogrammetry (Rottensteiner et al., 2014), laser scanning (Vosselman & Dijkman, 2001; Xiong et al., 2016), conversion from architectural models and procedural modelling (Julin et al., 2018).

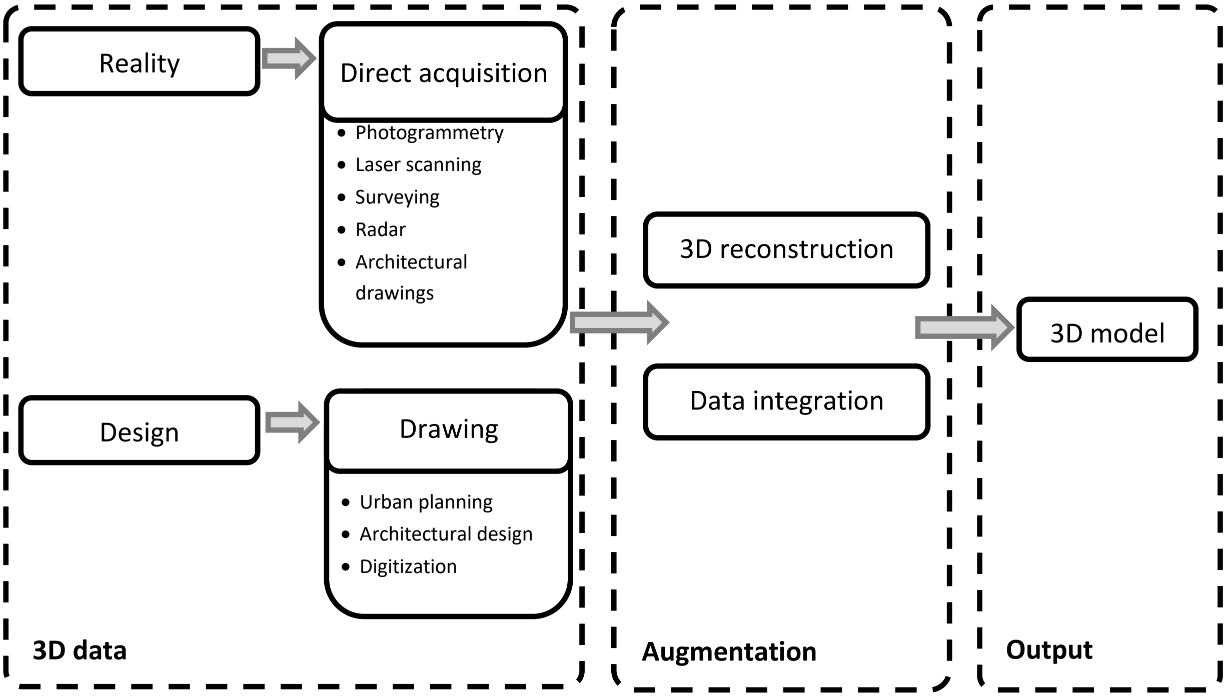

Figure 3. The acquisition process of 3D data and production workflow of the 3D model, adopted from Biljecki et al. (2016) and Stein & Tolpekin (2013).

2.1.2. Characteristics of 3D data

The 3D data used for this research is based on LiDAR and aerial photogrammetry. LiDAR surveys for height data collection have grown vastly. For example, the Netherlands has produced national airborne LiDAR point clouds and digital surface models (DSMs) at resolutions of 0.5m and 5m. This height data is collected from 1997 and it takes six years to collect the data for the whole Netherlands (Actueel Hoogtebestand Nederland, n.d.). The main characteristics of LiDAR data in the form of point clouds are an accuracy between 5 to 25 cm standard deviation for planimetric and 5 – 10 cm for the vertical accuracy (Kedzierski & Fryskowska, 2015; Oude Elberink & Vosselman, 2011); different resolution and characteristic gaps in data (strip offsets). This type of laser scanning allows to capture the object on the top plane, but not able to capture objects that are occluded or do not have a reflection properties such as water.

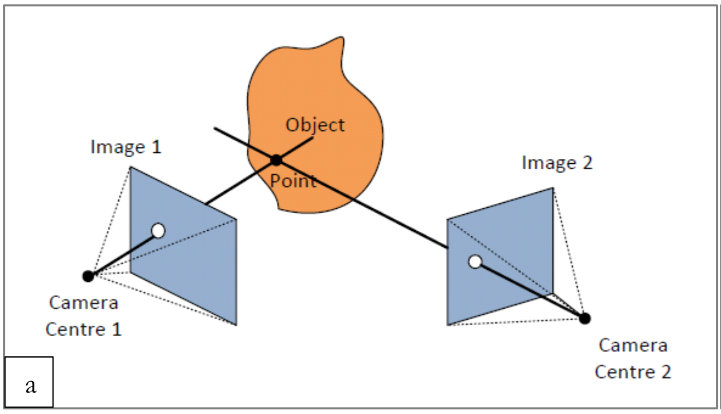

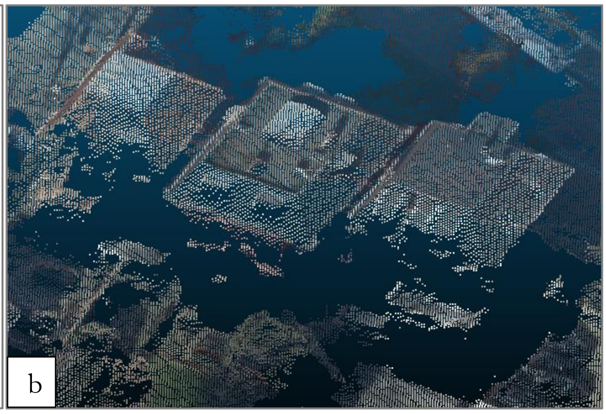

Figure 4. (a) Dense image matching process; (b) Point clouds obtained from DIM.

On the other hand, the Netherlands collects high-resolution aerial imagery every year for the production of stereo images and orthophoto mosaic (Beeldmateriaal Nederland, n.d.). These aerial images can be generated into point cloud through a dense image matching (DIM) process (Figure 4). This matching process obtains a corresponding point for every pixel in the stereo images and obtains depth to produce the height information (Kodde, 2016). The output of the matching process is a disparity image where the intensity is a measure for the height. This type of point cloud allows capturing any object from the top. However, this dataset is not publicly available.

2.1.3. Quality of 3D data

According to ISO 2:2004 (ISO, 2004), a standard is a *"document, established by consensus and approved by a recognized body, that provides, for common and repeated use, rules, guidelines or characteristics for activities or their results aimed at the achievement of the optimum degree of order in a given context"*. This standard can be achieved with a standardization process. Standardization is an activity to formulate, issue and implement standards (ISO, 2004). The benefit of this activity is an improvement of the suitability of products, processes and services for its intended purposes, facilitates product exchange and eliminates technical barriers. The standard serves to determine a level of quality. Quality is defined as the degree to which demands are met by a set of characteristics (ISO, 2013). In terms of geodata, those characteristics are called spatial data quality elements. Following ISO 19517:2013 (ISO, 2013), there are six elements for spatial data quality, shown in Figure 5. The six elements for spatial data quality are completeness, thematic accuracy, logical consistency, temporal quality, positional accuracy and usability element.

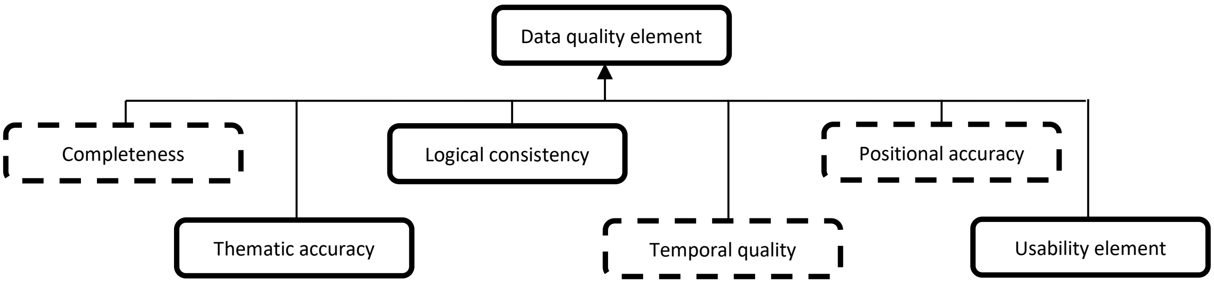

Figure 5. Overview of ISO 19517:2013 data quality elements. The focus of this research marked with dash outline.

The quality of 3D models can be analysed by determining the quality of input data (Oude Elberink & Vosselman, 2011; Ronnholm, 2011). From the six elements for spatial data quality, we selected on completeness, temporal quality, and positional accuracy, since they have a significant impact on the geometric aspect of 3D data. According to ISO 19517:2013, (1) completeness is defined as the presence and absence of features; (2) temporal quality is defined as the quality of the temporal attributes and temporal relationships of features and (3) positional accuracy is defined as the positional difference within a spatial reference system.

In terms of the input data that we use, completeness can be measured by answering the questions "how complete are the point clouds compared to building footprints?" or "is there any unmatched data?". Temporal quality can be measured from the metadata of each dataset and by a change detection process. In the metadata, we can see the information related to temporal quality; such as acquisition date. Positional accuracy can be measured from the density of the point cloud and by calculating the deviation between the dataset by comparing to the dataset which the positional accuracy is known.

2.1.4. Usage and benefits of 3D data

Compared to 2D, 3D data improves the communication process between users and the professionals in order to gain a better understanding of the presented information as stated by Kurakula & Kuffer (2008) and Onyimbi, Koeva, & Flacke (2018). The 3D model is an urban representation with a three-dimensional geometry with buildings as the main object of interest (Biljecki, Stoter, et al., 2015; Oude Elberink & Vosselman, 2011). The 3D models are mainly used for domain applications in environmental simulations and decision support (Biljecki, Stoter, et al., 2015), for instance in noise simulations (Kumar, Ledoux, Commandeur, & Stoter, 2017; Kurakula & Kuffer, 2008), solar irradiation (Alam, Coors, & Zlatanova, 2013; Biljecki, Heuvelink, Ledoux, & Stoter, 2018), real-estate(Toppen, 2016; Zhang, 2019) and sub-surface model (Ghodsvali, 2018) (for more applications see (Biljecki, Stoter, et al., 2015)).

2.2. Data integration

The fusion of LiDAR point clouds with DIM point clouds is popular (Kedzierski & Fryskowska, 2015; Ronnholm, 2011). This powerful method can combine the best of both, i.e. increasing the point density, although it might introduces noise or influence the positional accuracy.

Kedzierski & Fryskowska (2015) consider the integration of point clouds as the most detailed and accurate systems for acquiring 3D data. Integration of aerial images and laser scanner data was performed in Kaartinen et al. (2005). They evaluated the quality, accuracy, feasibility and economic aspects of semi-automatic building extraction derived from aerial imagery and laser scanning carried out by 11 experiments (Kaartinen et al. 2005). According to Kaartinen et al. (2005), laser scanning data is good to derive building heights, extraction of planar roof faces and roof ridges, while photogrammetry and aerial images are appropriate for the construction of outlines and lengths.

Another case of 3D data integration is shown in the work of Rottensteiner et al. (2014). In their research, the authors present two tasks, urban object detection and 3D reconstruction using the integration of two different point clouds, retrieved from DIM and laser scanning (Rottensteiner et al., 2014).

From the previous works mentioned, the main challenge when performing data integration is to correctly and accurately integrate the datasets when those data sets characterise different accuracy, density and content.

To perform the integration of point clouds, several methods have been developed, for instance, Matching Bounding-Box Centres Registration (Ahmad Fuad, Yusoff, Ismail, & Majid, 2018), Coherent Point Drift (CPD) (Myronenko & Song, 2010) and Normal-Distributions Transform (NDT) algorithm (Biber & Wolfgang, 2003). One of the widely used method to register two point clouds is the Iterative Closest Point (ICP) method (Gelfand, Ikemoto, Rusinkiewicz, & Levoy, 2003) which was first introduced by Besl & Mckay (1992). The principle of this relative positioning algorithm is to find corresponding points between two-point cloud datasets. The algorithm works by estimating a rigid transformation between points from the reference point cloud and points from the target point cloud. This algorithm implements nearest neighbours and Euclidean distance to estimate the closest point between the two points as correspondence points (Ahmad Fuad et al., 2018; Girardeau-Montaut, n.d.). According to Ahmad Fuad et al. (2018), this algorithm is the most suitable method to register point cloud dataset. Therefore in this study, we adopted this algorithm to register the DIM point cloud to the reference, the LiDAR point cloud. A major advantage of this relative positioning algorithm is, it reduces fieldwork to collect ground control features because only one data set, in this case, LiDAR, has to be georeferenced (Ronnholm, 2011).

The application of the ICP method has been used for the integration between airborne laser scanning (ALS) and terrestrial laser scanning (TLS) by Kedzierski & Fryskowska (2015) to obtain a complete 3D model. They focused on the processing of both data sets to create a uniform spatial coordinate system. Sirmacek & Lindenbergh (2014) assessed accuracy, advantages and limitations of point cloud generated using multi-view iPhone images and a TLS point cloud with this method.

2.3. 3D model and solar photovoltaic analysis

This section presents the definition of solar photovoltaic potential and the required information related to input data for calculating solar photovoltaic potential.

2.3.1. Definition of solar photovoltaic potential

Solar irradiation is the amount of solar energy (solar radiation emitted by the sun) received by the sun per unit area by a given surface (Biljecki, Heuvelink, Ledoux, & Stoter, 2015b). Solar radiation analysis is able to determine areas with maximum solar radiation exposure on the rooftop. The solar tools in GIS are able to analyze the effects of the sun over a specific geographic location with a time interval range. Nowadays, those tools can be easily found in nearly every GIS software, as elaborated by S. Freitas et al. (2015). Recognized from the explanations of Bódis, Kougias, Jäger-Waldau, Taylor, & Szabó (2019); Freitas et al. (2015); Mainzer et al. (2014) there are four factors to determine the type of potential, economy factor, panel performance, global irradiance, and geographic factor (Table 2).

Adopted from Izquierdo, Rodrigues, & Fueyo (2008), hierarchical potential methodology as follows. First is *physical potential*, which is the maximum amount of solar energy in a geographical region without considering any limitations (Freitas et al., 2015). However, another term is used for this level of potential, such as theoretical (Mainzer et al., 2014) and resource (Bódis et al., 2019), but the concept is the same. Second is the *geographical potential*, which considers the restrictions of the location (Freitas et al., 2015; Mainzer et al., 2014). The third is the *technical potential*, that takes into account the technical characteristics of the equipment, including the performance and efficiency of the photovoltaic modules (Bódis et al., 2019; Freitas et al., 2015; Mainzer et al., 2014). Interestingly, according to Mainzer et al. (2014), the term geographical and technical potential has been used interchangeably and is widely employed in the assessment of photovoltaic potentials. However, we argue that those two potential are two different types of potential and should not be used interchangeably because different factors are taken into account during analysis which could lead to confusion. The last is the *economic potential*. It takes economic factors into account such as return on investment, payback time, and production revenue (Bódis et al., 2019; Mainzer et al., 2014; Paardekooper, 2015).

The hierarchy used in this research comprises two levels. First, the physical potential to calculate the solar irradiation for the whole study area. Second, we calculate the geographic potential to focus on finding locations where energy can be captured. The last two levels, namely technical potential and economic potential, are not included in this research as the main emphasis is on the evaluation of the quality of the input data for the analysis.

Table 2. Definition of different types of solar potential.

Factor	Type of potential	Elaboration	Author
Global irradiance	Physical potential	*"Encompasses the maximum amount of solar energy that can be received in a certain area."*	Freitas et al. (2015, p.916)
		"All the available irradiation in a geographical region without considering any geographical or technical limitations."	Mainzer et al. (2014, p.717)
		"for photovoltaics, the annual incident solar radiation and other relevant environmental parameters such as ambient temperature and wind speed."	Bódis et al. (2019, p.2)
Geographic factor	Geographical potential	*"That fraction of the theoretical potential that is utilizable, i.e. because the land or area is available and suitable."*	Mainzer et al. (2014, p.717)
		"Geographic potential is calculated by gradually excluding the zones reserved for other uses, restricting the locations where solar energy can be gathered."	Freitas et al. (2015, p.916)
Panel performance	Technical potential	*"Available suitable surface area, system technical performance, sustainability criteria if applicable."*	Bódis et al. (2019, p.2)
		"The irradiation that is technically usable taking also into account the efficiency of photovoltaic modules."	Mainzer et al. (2014, p.717)
Economy factor	Economic potential	*"deployment considering competition with other sources, policies, legal-permitting aspects, incentives, socio-cultural factors, etc."*	Bódis et al. (2019, p.2)
		"technology costs avoided supply costs."	Bódis et al. (2019, p.2)
		"share of technical potential economically usable from an investors' or macroeconomic point of view."	Mainzer et al. (2014, p.717)

2.3.2. The general approach to estimate solar photovoltaic potential

According to Freitas et al. (2015), a sequential approach is required to estimate the solar photovoltaic potential, shown in Figure 6.

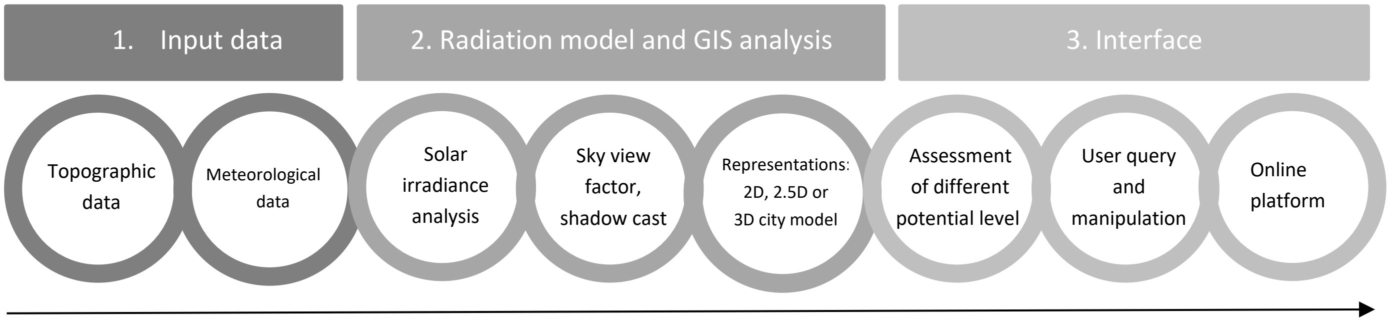

Figure 6. The sequential process to assess solar photovoltaic potential, adapted from Freitas et al. (2015).

In general, the approach consists of three steps. First, information regarding the features and surroundings of the area that can be obtained from several techniques. Second, a solar radiation model with GIS analysis is used. For this step, the 3D input data plays role as the main input data as urban representation. Third is the visualization of the output.

2.3.3. Choosing the input data for solar photovoltaic analysis, 2.5D or 3D?

The main component of the solar photovoltaic analysis is the geographic location, including height information and urban element. Geodata in 2.5D or 3D gives information such as elevation, orientation (slope and aspect), and shadow from surrounding features. In general, the 2D data is insufficient to provide that information; thus, geodata in 2.5D or 3D is needed (Freitas et al., 2015; Machete, 2016).

Compared with 2D data that is embedded in a 2D space (x, y), 2.5D is embedded in a 3D space whereas each location (x, y) is assigned to one height (z). From the acquisition process explained in Section 2.1.1, instead of augmented and generated into a 3D model, the collected data is discretised into grid or raster form (J. P. Wilson, 2012). The outcome of this process is a Digital Terrain Model (DTM) or a Digital Surface Model (DSM).

In contrast, 3D data provide for each location (x, y) as well as its corresponding height (z). From the result of the acquisition process and reconstruction process explained in Section 2.1.1, a 3D model allows representing an urban scene with volumetric forms. The difference between these two representations is illustrated in Figure 7.

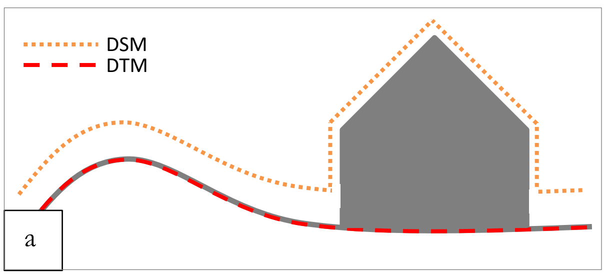

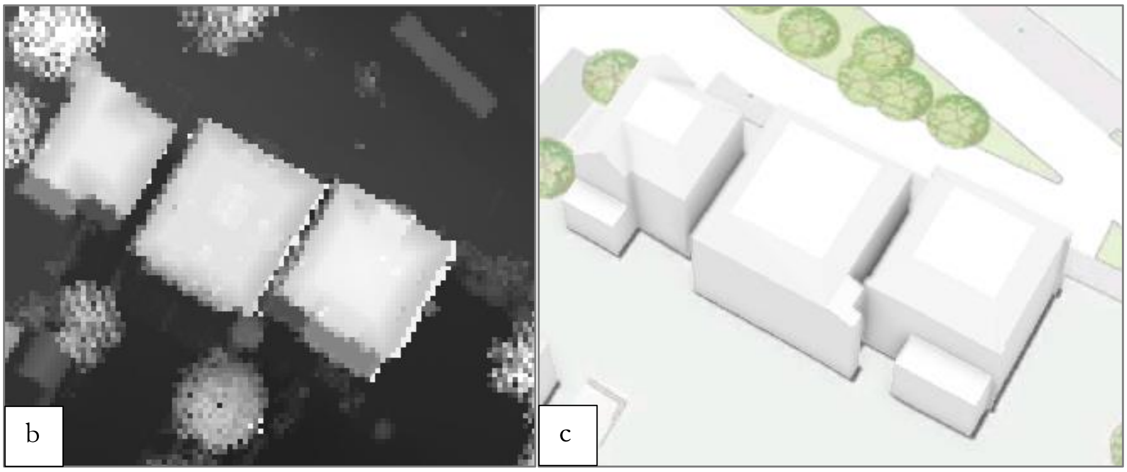

Figure 7. (a) Difference between DTM and DSM; (b) 2.5D representation, DSM (c) 3D representation, 3D model.

Considering the explanations above, the question arises: *when are 2.5D and 3D data supposed to be used for such analyses?*

Biljecki et al. (2015) classified two types of use cases for utilizing GIS analysis and 3D model into non-required visualization use cases and visualization required use cases. The case of solar photovoltaic analysis belongs to the non-required visualization use case (Biljecki, Stoter, et al., 2015). In the context of 3D building models, Biljecki, Ledoux, & Stoter (2017) and Peronato, Bonjour, Stoeckli, Rey, & Andersen (2016) argue that the use of a more detailed roof model, (i.e. a higher level of detail (LOD)) provides a better result for spatial analysis such as calculating the photovoltaic potential. However, using more detailed roof model are likely more complex and involve higher costs both in time and money for large scales (Biljecki et al., 2017; Peronato et al., 2016).

Machete (2016) and Peronato et al. (2018) observe distinct differences in the utilization of 2.5D and 3D as input data for solar photovoltaic analysis. According to their studies, a 2.5D representation is sufficient for solar photovoltaic potential analysis on the roof while a 3D representation is useful for solar photovoltaic potential analysis on the façade (Machete, 2016; Peronato et al. 2018).

Important theme emerges from the studies discussed is the use case of solar photovoltaic potential benefited from the use of a more detailed roof model. However, we argue that the choice of both representations can be justified with regard to the limitation of the software for solar radiation analysis, the impact on the result and the users' needs. Therefore to answer the question, *when are 2.5D and 3D data supposed to be used for such analyses?* we investigated the usability of 3D model as input data for solar radiation analysis explained in section 3.6.

2.4. Summary

Physical reality can be represented using 3D models from different data sources. The most common approach to collect 3D data uses aerial or terrestrial surveying. Different acquisition techniques produce different data characteristics. Point clouds derived from LiDAR are irregular, have multiple returns, but are not able to capture objects that are occluded or do not have reflection properties such as water. On the other hand, the point cloud produced from DIM processes are regular. These two types of 3D data are commonly integrated to generate a more detailed and accurate 3D model. The 3D models, are mainly used to simulate environmental problems as a part of decision support. In the case of solar photovoltaic, the literature review revealed that the not only 3D models but also 2.5D are used as input. However, the usability between these two are still debatable.

3. METHODOLOGY

This chapter introduces and elaborates on the methods applied for this research. The structure of this chapter consists of seven sections. The overall methodology of the study is shown in section 3.1. The following sections 3.2– 3.6 elaborate on the study area and on the implementation of the findings from the literature review to answer sub-objective 1, to investigate the characteristics of the input data, and sub-objective 3, to develop a 3D model to estimate the potential of a solar photovoltaic installation. At the end of the chapter, section 3.7 summarizes the used methods in this research.

3.1. The overall approach of the study

The overall approach of this study is a mixed qualitative-quantitative method (Figure 8). Per sub-objectives, the tasks are identified, and the approaches are chosen to address the sub-objective and related questions of this study. Following statements explain the choice rationale.

Sub-objectives	Tasks	Data collection	Data process & analysis	Methods
Investigate the characteristics and content of the input data	Identify 3D data characteristics and utilization	Literature review	Pre-processing data	Metadata examination Visual check data completeness
	Define data quality elements	Literature review		Point density calculation Point cloud classification
Prepare unified data that satisfy the user needs for 3D models	Data integration	Literature review		Point density registration
	Identify user perspectives	Semi-structured interview	Content analysis	
Develop a 3D model to estimate the potential of solar photovoltaic installation	3D model generation	National geodatabase and registers extraction	Construct a 3D model	Semi-automatic 3D model construction with RANSAC
	Solar photovoltaic potential analysis	National geodatabase and registers extraction	Solar radiation analysis	
	Model evaluation	Focus group discussion	Content analysis	

Qualitative | Mix method | Quantitative

Figure 8. Overall research approach.

This study requires information related to 3D modelling and solar photovoltaic and also takes the users' perspective into account. Literature review, semi-structured interview and focus group discussions are appropriate methods for knowledge gathering and data collection. The semi-structured interviews are able to support information regarding user perspectives. Furthermore, focus group discussion involving experts is chosen to evaluate the fitness for the purpose of the output.

The data process and analysis phase include both qualitative and quantitative approaches. Methods that are applied in this phase are based on the dimensions and technique identified from the literature review in the data collection phase. For the quantitative approach, data pre-processing was done to calculate point density, to classify point clouds and to register point clouds. Moreover, the result of pre-processing is used to generate the 3D model and solar radiation analysis. For the qualitative approach, the result of the semi-structured interview and focus group discussion are analyzed with a content analysis technique by organizing the information into categories. Illustrated in Figure 10 is the workflow of this study. Further explanation of each process is explained in section 3.3– 3.6.

3.2. Study area

The study area was selected to be the inner city of Zwolle, at the province Overijssel, the Netherlands (Figure 9. Location of the study area: (a) city of Zwolle and (b) subset of the study area in the 3D model.). The inner city of Zwolle is characterized by mixed residential and commercial buildings with diverse structures. Therefore, it is a suitable study area for experiments with 3D data. The area is protected in regards to solar photovoltaic installation because it has old architecture and historical buildings. Also, the municipality of Zwolle applies the line of sight regulation from the public area when applying solar photovoltaic installation (Boschman, 2017). Line of sight regulation is a regulation that determines whether a given point is visible from another point. The line of sight regulation protects the view of the historical city and its characteristics, by disallowing any changes to buildings that are in the line of sight from the public road.

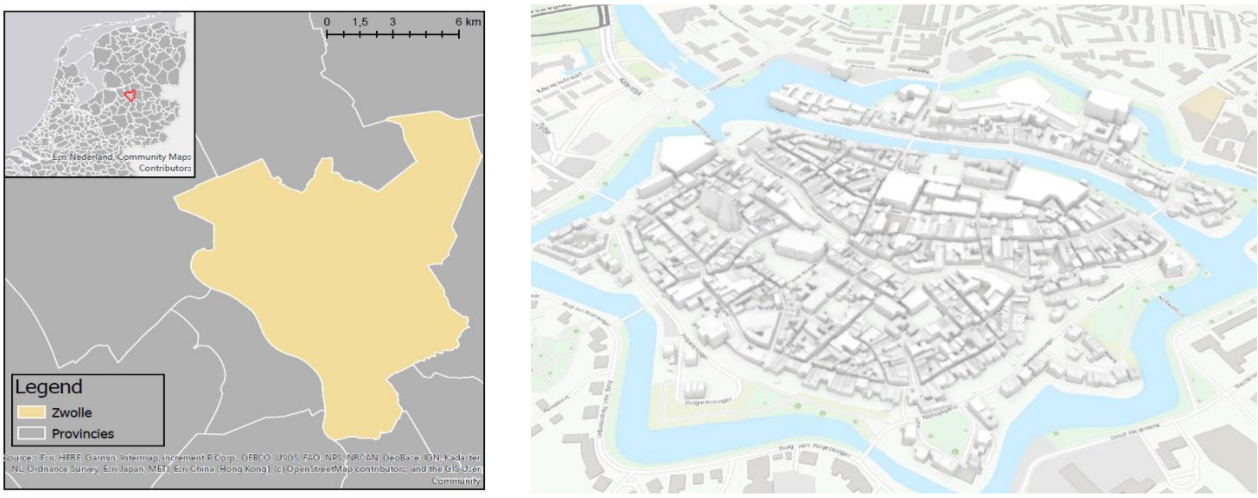

Figure 9. Location of the study area: (a) city of Zwolle and (b) subset of the study area in the 3D model.

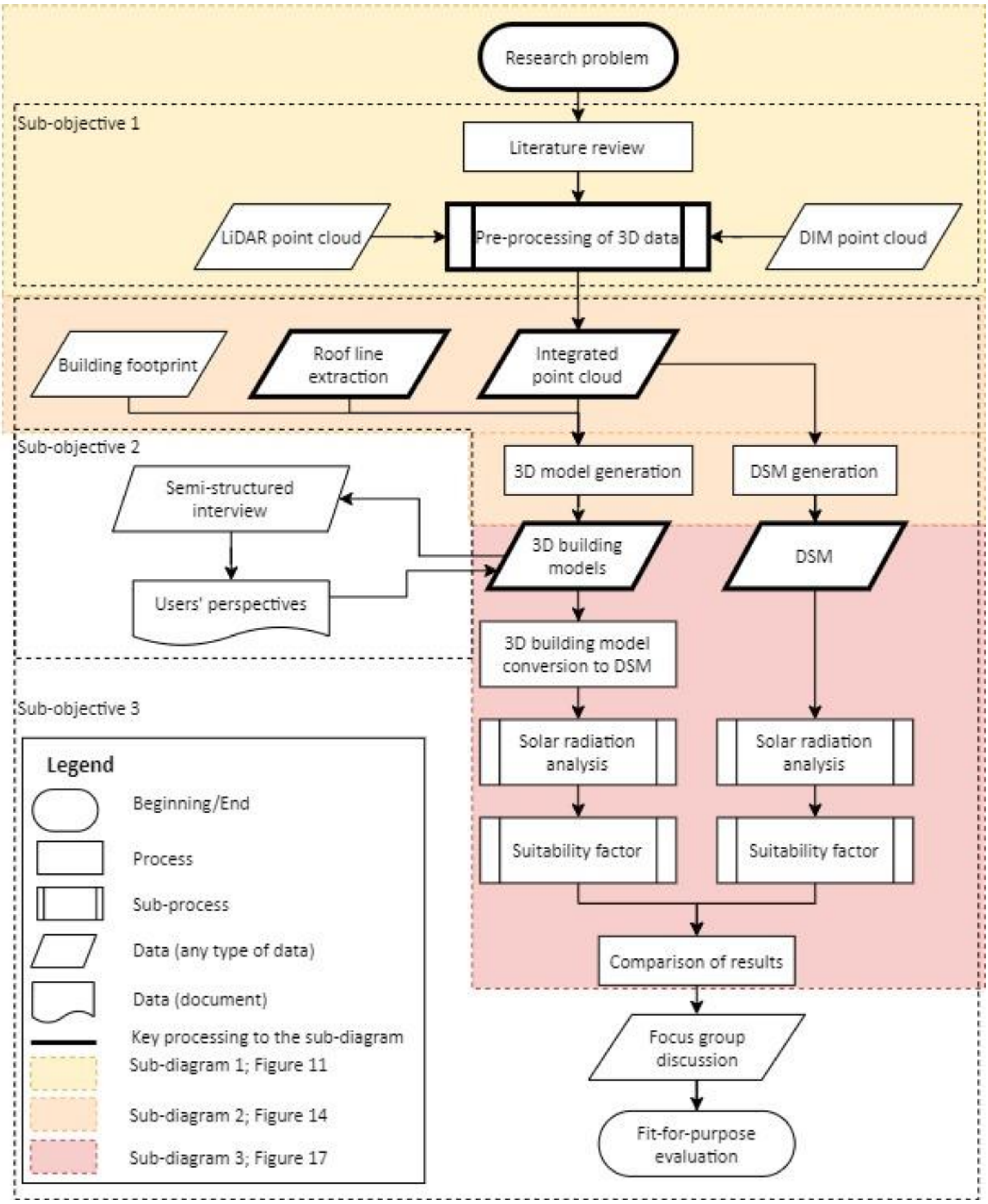

Figure 10. Implemented methods and techniques workflow of this study.

3.3. Pre-processing of 3D data

The requirements for the pre-processing of 3D data were derived from findings from the literature review. Obtained from the literature review, there are six elements to define spatial data quality. In this research, we focus on three elements, *completeness, temporal quality* and *positional accuracy*. These elements were chosen because they have a significant impact on the geometric aspect of 3D data. These elements were adapted into several processes. These processes consist of metadata examination, visual data completeness inspection, point density calculation, point cloud classification and point cloud registration. The output of these multiple processes is an integrated point cloud (Figure 11). The data used for this research is the LiDAR point cloud, and DIM (DIM) point cloud. These datasets are provided by Kadaster. Metadata from the data were examined to check the temporal resolution, format, fields attached, positional accuracy and acquisition process. Besides metadata, this information is also acquired through discussion with people at Kadaster, from the internet and *productspecificatie*[3]. Table 3 presented the description of the datasets used for the whole research

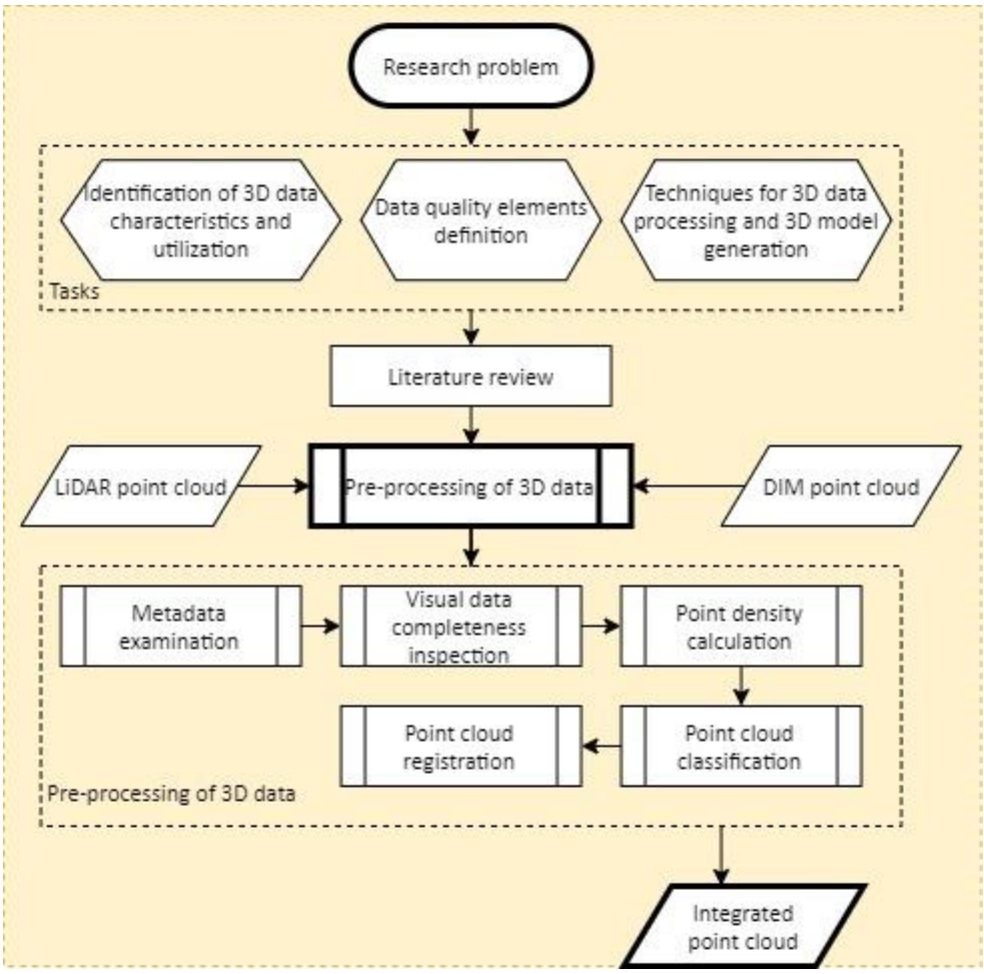

Figure 11. Workflow diagram for pre-processing the LiDAR point cloud and DIM (DIM) point cloud. This is part of Figure 10.

Table 3. Data description.

Dataset	Data source	Date of release	Format	Fields/information
Building footprints (BAG)	PDOK	January 2020	Vector - footprints	See Ministerie van Binnenlandse Zaken en Koninkrijkrelaties, (2018)
LiDAR point clouds(AHN3)	PDOK	2016	Point cloud	Point format, Z minimum and Z maximum, point count, return number, the total number of returns.
DIM point clouds	Kadaster	2019 winter images	Point cloud	Derived from aerial winter imagery.

The building footprints are maintained and extracted manually from aerial imagery by each municipality(Figure 12a). This vector data is distributed to Kadaster and made available to the public[4]. According to the metadata of Actueel Hoogtebestand Nederland (n.d.), the LiDAR point clouds (Figure 12b) were collected from laser altimetry from aircraft. The flights took several weeks (influenced by weather and flight permissions). For AHN3 in total, the data was captured from 2014 – 2019 (Actueel

[3] https://www.geobasisregistraties.nl/documenten/publicatie/2018/03/12/catalogus-2018
[4] https://www.pdok.nl/introductie/-/article/basisregistratie-adressen-en-gebouwen-ba-1

Hoogtebestand Nederland, n.d.). The vertical accuracy for AHN3 is 5cm stochastic and 5cm systematic, the planimetric accuracy is 8cm stochastic and 5cm systematic (Actueel Hoogtebestand Nederland, n.d.). The DIM point cloud (Figure 12c) was derived from aerial winter imagery. The ground pixel resolution of this image is between 4 – 10cm, with an overlap of 60% and 30%. The output is a 3D point cloud, which was used in this research.

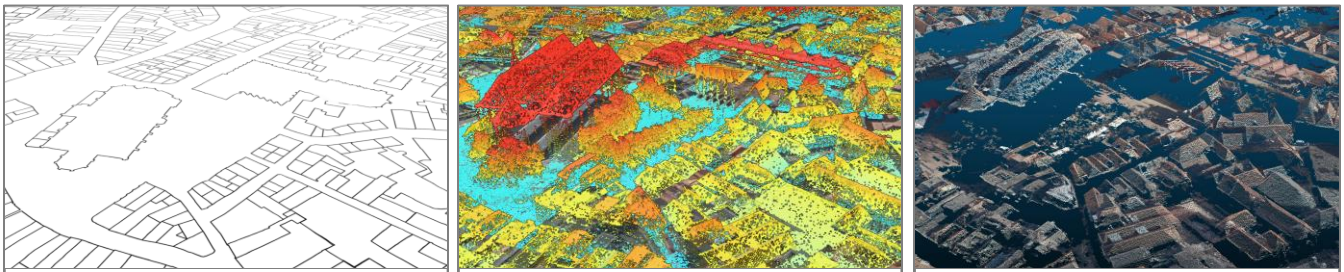

(a) Building footprints | (b) LiDAR point cloud | (c) Dense image matching point cloud

Figure 12. The geodata being used in this research, building footprints, LiDAR point cloud and DIM point cloud.

3.3.1. Visual check data completeness

Completeness can be measured by comparing datasets to true reference (see section 2.1.3). This phase is to check if the point cloud datasets used are complete or if there is an obvious lack of completeness in the study area. Therefore, for this phase, a visual inspection by comparing two datasets was done as the first screening. Afterward, statistic calculation with a point to point distance calculation was carried out as part of the point cloud registration process. Two additional datasets as visual ground truth to detect changes were also used: Cyclomedia[5] and Google Maps[6]. These two are the providers for street-level imagery data. See section 3.3.4 for the technique of point cloud registration and section 4.1.3 for the result of the point cloud registration and visual check with the additional datasets.

3.3.2. Point density calculation

The point density is calculated using LAS Dataset tools from ArcGIS Pro. The output of this tool is point spacing. According to Esri, (n.d.), point spacing is not the same as point density. Point spacing (PS) is defined as linear units per point, while point density (PD) is defined as points per square unit area. To convert point spacing to point density, Equation 1 is applied. A higher point density means lower values for point spacing. The result of this calculation is presented in section 4.1.2.

$$Point\ density = \frac{1}{(Point\ spacing)^2} \qquad (1)$$

Equation 1. Formula to calculate point density from point spacing, adopted from Esri, (n.d).

3.3.3. Point clouds classification

Point clouds classification is a process to automatically assign points to predetermined classes. The American Society for Photogrammetry & Remote Sensing (ASPRS) (2011), has defined a standard classification scheme (Table 4). The point cloud datasets used in this research are successfully classified into four classes code value: unclassified (1), ground(2), building (6), water (9). The result of the classification process is elaborated in section 4.1.2. Afterward, a separate dataset is created by subtraction of the points classified as a building because the main interest of this research are buildings.

[5] https://www.cyclomedia.com/en
[6] https://www.google.com/maps

Table 4. ASPRS standard LiDAR classes.

Classification value	Meaning
0	Created, never classified
1	Unclassified
2	Ground
3	Low vegetation
4	Medium vegetation
5	High vegetation
6	Building
7	Low point (“low noise”)
8	High point (typically “high noise”)
9	Water
10	Rail
11	Road surface
12	Bridge deck
13	Wire – guard
14	Wire – conductor (phase)
15	Transmission tower
16	Wire- structure connector (e.g. insulator)
17	Reserved
18 – 63	Reserved
63 – 255	User definable.

3.3.4. Point clouds registration

Adopting from previous work elaborated in Section 2.2, we used the ICP algorithm to register the two point clouds dataset. This process was done in CloudCompare software. In principle, the algorithm steps are as follows (Figure 13):

1. For each point in the source (DIM) point cloud, find the closest point in the reference (LiDAR) point cloud.
2. Estimate the combination of rotation and translation with a mean squared error function that will best align each source point to find its match.
3. Transform the source points using the obtained transformation matrix.
4. Iterate the steps.

The output of this algorithm provides a transformation matrix and a roughness value. This transformation matrix is used to transform the source point into a reference point. The roughness value (mean and standard deviation) is equal to the distance of the point and the best fitting plane in the neighboring points (Girardeau-Montaut, n.d.; Sirmacek & Lindenbergh, 2014). This value represents the distribution of the distances calculated between two-point cloud datasets. The result of this process is presented in section 4.1.3.

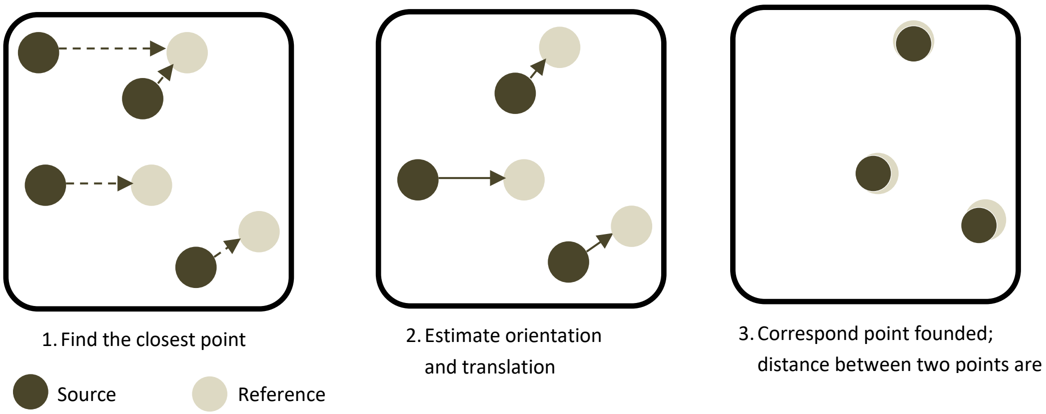

Figure 13. Principle of the ICP algorithm.

3.4. The 3D model generation

The 3D model was generated semi-automatic with the integrated point cloud generated from section 3.3, building footprints (BAG[7]) and rooflines (Figure 14). Kadaster has available datasets of rooflines that are manually digitized. However, there are some places in the study area where the rooflines are incomplete. We digitized the rooflines to this missing area following the same procedure of the available rooflines datasets, which is manual digitizing from true orthophoto from aerial imagery. The rooflines are illustrated in Figure 16. The rooflines consist of two types of lines: height jump and ridgeline. Height jump is the edge of roof faces that have a significantly different height, while a ridge line is a line formed along the rooftop.

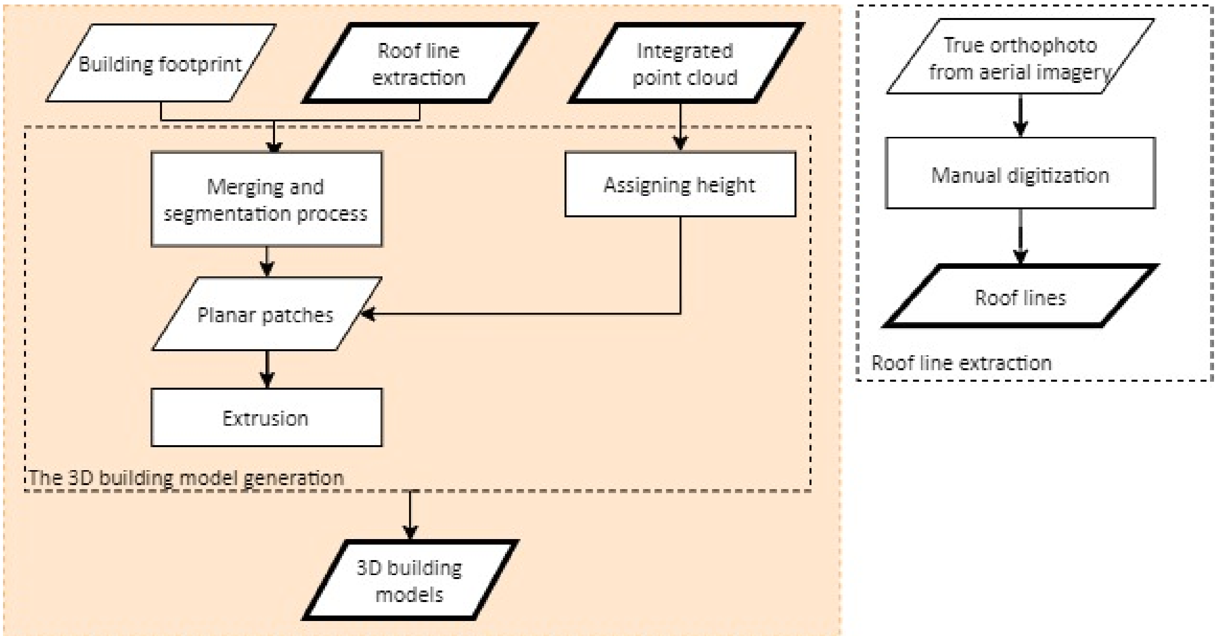

Figure 14. Workflow diagram for generating the 3D model. This is part of Figure 10.

The sequence of the 3D model construction is illustrated in Figure 15. The 3D model construction started with merging and segmenting rooflines and building footprints (Figure 15a) while maintaining the building identifier (ID). The result of this step is planar patches (Figure 15b). After the planar patches are produced, the integrated point clouds are assigned to the planar patches (Figure 15c). Afterward, each planar patch was reconstructed following the height and the slope direction obtained from the integrated point clouds. The process was carried out using the RANSAC algorithm (Fischler & Bolles, 1980) to segment the point clouds into planes.

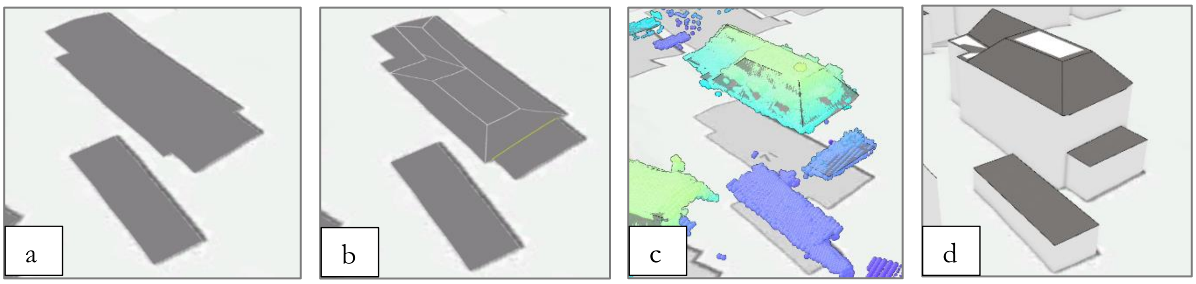

Figure 15. The sequence of 3D model generation. The first image (a) is the building footprints. The rooflines consist of ridge lines (white), and height jumps (yellow) were merged, and the building footprints were segmented—this process resulting in planar patches (b). The point clouds were continuously iterated with the RANSAC algorithm to fit the candidate shape and the confidence parameter until reaching the consensus, shown in grey color on picture (c). Afterward, the building footprints were merged again with the segmented roof from the picture (c) to generate a full 3D model shown in the picture (d).

[7] https://www.pdok.nl/introductie/-/article/basisregistratie-adressen-en-gebouwen-ba-1

RANSAC algorithm is well known to detect primitive shapes in both 2D and 3D (Schnabel, Wahl, & Klein, 2007). This algorithm was introduced by Fischler & Bolles (1980) and consisted of three parameters: (1) error tolerance to determine whether a point is compatible with the fitting plane or not, (2) the number of subsets to try, (3) the threshold. The algorithm starts by randomly selecting a minimal subset of *n* points and estimating the corresponding fitting shape parameters. The remaining points are tested with the resulting candidate shape to see how many points fit the candidate shape. After a certain number of iterations, the shape that has the largest percentage of inliers is extracted, and the algorithm continues to process the remaining data. The result of this step is floating planes, which were combined with the corresponded extruded building footprints (Figure 15a) to produce a full 3D model (Figure 15d).

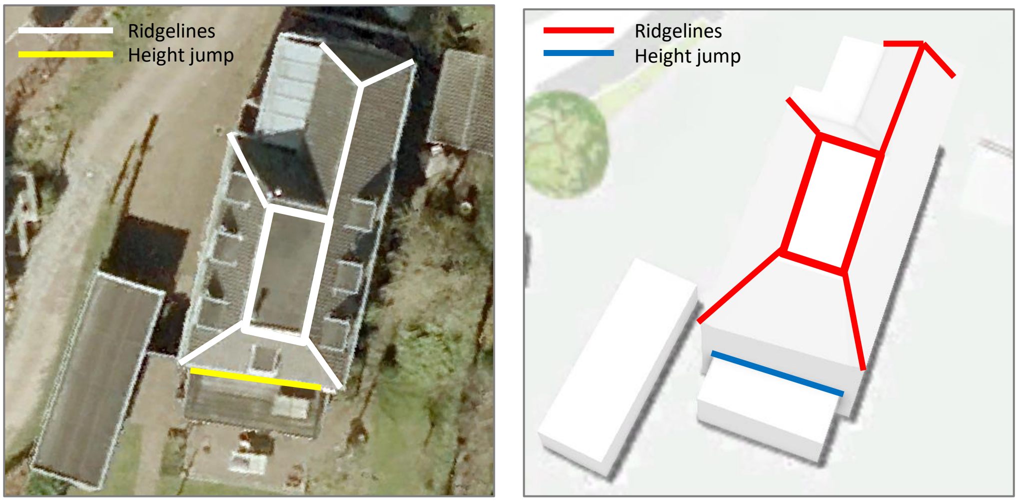

Figure 16. Illustration of ridgeline and height jump in 3D models. Left is from the aerial imagery, and right is from the 3D model.

3.5. Application for solar photovoltaic potential

The solar photovoltaic potential was done in two steps. First, 3D models were converted into raster. Second, the solar potential estimation was calculated using the Area Solar Radiation tool (Figure 17. Workflow diagram for calculating solar radiation to estimate the solar photovoltaic potential. This is part of Figure 10.). As explained in section 2.3.1, for geographic potential, the main criteria to determine the suitable solar photovoltaic are solar irradiation, slope, and orientation. The 3D models were converted into raster because the main input of the Area Solar Radiation tool in ArcGIS is DSM. This tool accounts for atmospheric effects, roof slope, roof orientation and effects of shadow cast. Afterward, a raster was taken as output with pixel values in units of Wh/m². The solar radiation was calculated through a 1-year simulation of solar irradiation on rooftops.

To investigate the influence of pixel resolution, we converted the 3D models into rasters with different pixel sizes, 0.2m and 0.5m. Moreover, to assess the usability of using 3D models, we created another DSM raster from the integrated point cloud (section 3.3.4) as another input for solar irradiation calculation. Besides being part of the experiment, the objective of using DSM raster from the integrated point cloud is to see the improvement of the new methodology, because using DSM from the LiDAR point cloud is the current workflow that is implemented at Kadaster.

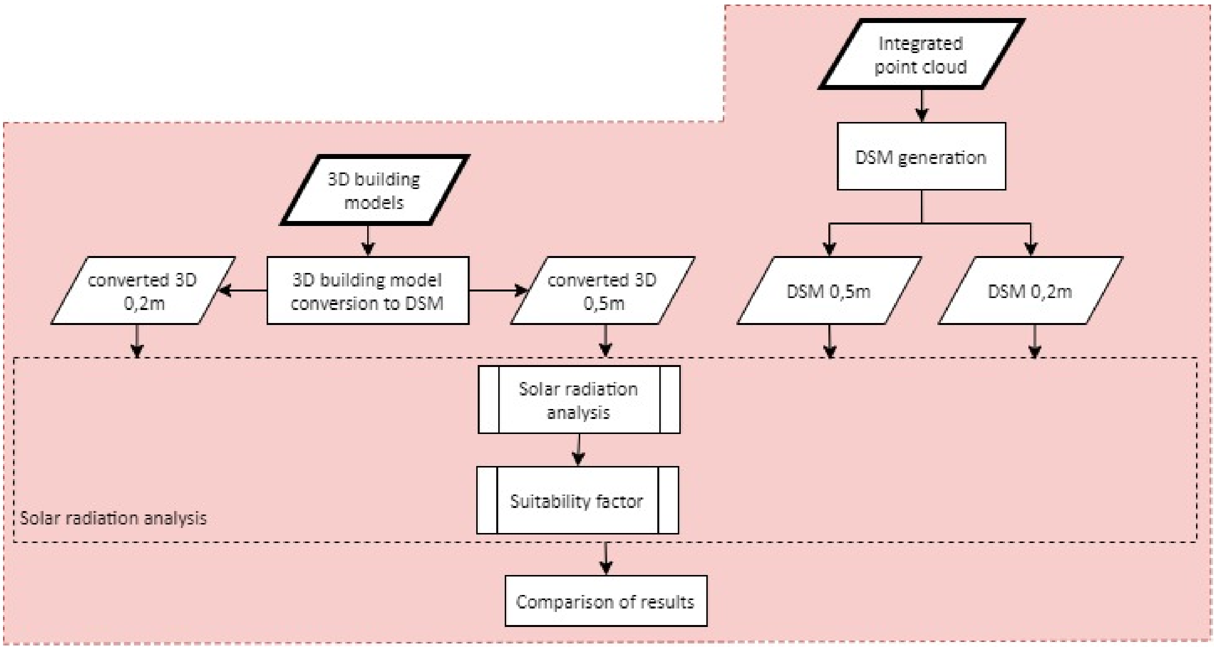

Figure 17. Workflow diagram for calculating solar radiation to estimate the solar photovoltaic potential. This is part of Figure 10.

3.6. Collecting data about the end-users' perspective

Besides the technical and data requirements, an important additional perspective in this study is the perspective of the end-users of the data. Semi-structured interviews and focus group discussion have been conducted to gauge their opinions. The objective of the semi-structure interview was to gather the required information needed related to solar photovoltaic analysis and to identify the compliance between the user requirements and the input data. The objective of the focus group discussion was to evaluate the model's fitness to the application of solar photovoltaic potential.

3.6.1. Semi-structured interview

The advantages of a semi-structured interview are its usefulness in gaining attitudes and opinions while retaining the possibility of discovering previously unknown issues (Wilson, 2014). The flexibility to add follow-up questions can help the interviewer to obtain detailed insight (Bryman, 2012; Zhang, 2019). The common technique for a semi-structured interview is the use of open-ended questions. Such questions allow to adapt questions to the interviewees' level of knowledge and understanding of the issues (Bryman, 2012).

There was no fixed number set of how many interviewees are needed in this research. However, the rule of thumb is when the given information starts to repeat itself, then the number of interviewees is enough (Toppen, 2016). Five experts were approached for the participation of whom four were willing to participate. The interviewees were experts from different backgrounds; municipality (Interviewee 1), solar analysis provider (Interviewee 2), land-mapping agency (Interviewee 3) and academia (Interviewee 4) (Table 5. Interviewees' background). These experts represent different knowledge areas related to solar photovoltaic analysis. The objective of these interviews was to obtain the professionals' personal opinions, knowledge and experiences with the use case. The interview was recorded and transcribed after the interview. The questions are shown in the Appendix.

Table 5. Interviewees' background

Interviewee	Background
Interviewee 1	Municipality from smart community department
Interviewee 2	Solar analysis provider

Interviewee 3	Land-mapping agency
Interviewee 4	Academia

3.6.2. Content analysis for the semi-structured interview

The interviews were held in different moments, depending on the schedule of each interviewee. These interviews were done at the start of this research. The transcription result is coded into seven dimensions, as shown in Table 6. Dimensions applied for content analysis for the semi-structured interview.These dimensions are defined to extract relevant information from the interview. According to Bryman (2012), content analysis helps to obtain a transparent result. The method supports that the results are replicable and support follow-up studies.

Table 6. Dimensions applied for content analysis for the semi-structured interview.

Dimension	Rationale
Background of work	To understand the background knowledge of the interviewee, which could influence his/her answers towards the interview questions.
Users	To identify the type of users from each interviewee.
Information needed for estimating solar photovoltaic	To identify the interviewee's considerations and influential factors that should be used in the calculation for estimating solar photovoltaic potential.
Additional data that they collect themselves	To identify additional data used in the interviewee's calculation of estimating solar photovoltaic potential, besides publicly available data.
Data used by the interviewee for solar photovoltaic potential estimation	To identify data type, format and suitability criteria used in their calculation for estimating solar photovoltaic potential.
Comments on standardization model	To understand the demand for establishing a standard model for estimating solar photovoltaic potential.
Comments on quality of currently publicly available data (BAG and AHN)	To understand the shortcomings of publicly available data that influence the estimation of solar photovoltaic potential.

3.6.3. Focus group discussion

Focus group discussion is an approach to observe the discussion and response of people on a particular, fairly tightly defined topic with several participants (Bryman, 2012). In the research, the participants were six experts in 3D modeling, point cloud and familiar with the solar photovoltaic application. The participants were selected with purposive sampling. The motivation for doing this focus group discussion is to evaluate the fitness of the model to the application of solar photovoltaic potential. This focus group aims to assess if the result of the 3D model obtained with the presented method is fit for the purpose. The perceived quality of the 3D model of the six participants was measured using qualitative indicators that include fit-for-purpose, general validation statements, and data integration. The session was started with an introduction about the research with presentation and video, followed by filling the questionnaire[8] (see Appendix for the questions and link to the video). The perception was measured on a scale of 1 (strongly agree) to 5 (strongly disagree), or no response, followed by several open questions. At the end of the session, we presented the outcome of the questionnaire to facilitate discussion between participants. The session was recorded, transcribed and analyzed with content analysis (Table 7. Dimensions applied for content analysis for focus group discussion.. The questions are attached in the Appendix and the results presented in section 4.5.

[8] We planned to have the focus group discussion offline. But due to the measures of the Dutch government in response of COVID-19 outbreak, we held the focus group discussion online.

Table 7. Dimensions applied for content analysis for focus group discussion.

Dimension	Rationale
The converted 3D model provides clear visualization for solar photovoltaic analysis.	To evaluate the presented method, ease the communication process for presenting the result of the solar photovoltaic analysis.
The converted 3D model provides the required information for solar photovoltaic analysis.	To evaluate the presented converted 3D model fulfilled the required information following the criteria obtained from the semi-structured interview
The 3D model could be adapted for other applications.	To evaluate the presented converted 3D model suits for other application than solar photovoltaic analysis.
The integration of the point clouds improves the data completeness element.	To assess the integration of LiDAR point clouds and DIM point clouds, compensate the omitted object in the dataset due to the properties of the LiDAR point clouds.
The integration of the point clouds improves the temporal quality element.	To assess the integration of LiDAR point clouds and DIM point clouds, compensate the changed and not acquired object due to the acquisition time of the LiDAR point clouds.
The integration of the point clouds improves the positional accuracy element.	To assess the integration of LiDAR point clouds and DIM point clouds positional accuracy close to the respective relative position of LiDAR point clouds.
List of improvements for the 3D model.	To evaluate the visualization of the presented 3D model closes to the perceived as reality.

3.7. Summary

This research carried out a mixed approach to gather and process the data. In overview, the methodologies applied were data collection, data processing and data analysis. Data collection consists of a literature review, data retrieval from national geodatabase and registration, semi-structured interviews, and a focus group discussion. Data processing and analysis consist of pre-processing of the 3D input data, 3D model generation, solar photovoltaic potential analysis, and content analysis for the semi-structured interviews and focus group discussion. The insights obtained from the literature review were applied to the pre-processing steps that consist of a visual check for data completeness, point density calculation and classification for LiDAR point cloud and DIM point cloud. In the end, both point cloud datasets were registered with the ICP algorithm resulting in the integrated point cloud. The 3D model was generated using the RANSAC algorithm with the integrated point cloud, building footprints and rooflines as our input data. The insights obtained from the semi-structured interview were applied to the solar photovoltaic potential analysis. The results of the solar radiation analysis were evaluated by means of a focus group discussion. The objective of the focus group discussion was to evaluate the fitness to the purpose of the model.

4. RESULT AND DISCUSSION

The methodology and its implementation are presented in this thesis allow to investigate the standardized 3D input data for solar photovoltaic potential. This chapter discusses the results found from the implemented methodologies in Section 4.1-4.5.

4.1. Result of the pre-processing of the 3D data

This section elaborates the result of pre-processing 3D data. The 3D data used in this research is the DIM point cloud and LiDAR point cloud. The process consists of metadata examination, visual check for data completeness, point density calculation, point cloud classification and point cloud registration resulting in the integrated point cloud.

4.1.1. Point density calculation

For the showcase point cloud, the DIM point cloud contains 19,036,479 points before classification and removing outliers. In the LiDAR point cloud, before classification and removing outliers, it contains 1,078,247 points, for the same area. The results of the calculated point spacing following Equation 1 are shown in Table 8. The result indicates that the LiDAR point cloud has less point density than the DIM point cloud.

Table 8. LAS file properties.

LAS File	Point count	Point spacing	Point density	Z min	Z max
LiDAR point cloud	15,078,247 pts	0.24 m/point	17 points/m^2	-1.014 m	78.522 m
DIM point cloud	19,036,479 pts	0.216 m/point	21 points/m^2	-20.119 m	75.305 m

4.1.2. Point cloud classification

The classification process started with ground classification and followed with classifying building rooftop points. Because the main interest in this research is the buildings, this process also removes noise from the point cloud. Class code values of 0 (never classified), 1 (unclassified), and 6 (building) are evaluated to determine if those fit the characteristics of a building rooftop. If they do not meet the criteria, then point clouds will be assigned to a class code value of 1 (Esri, n.d.). Both point clouds were classified into four classes code values: (1) unclassified; (2) ground; (6) building; (9) water.

Next, each point cloud was thinned to extract code class value 6 (building) and to derive a consistent density. However, after visual inspection, both point clouds contain false negative (Figure 18). The method recognizes boats as buildings; this false negative caused by the definition of the smallest area size of the building during the classification process. Therefore, the false-negative objects were selected manually and reclassified to code class 1 (unclassified).

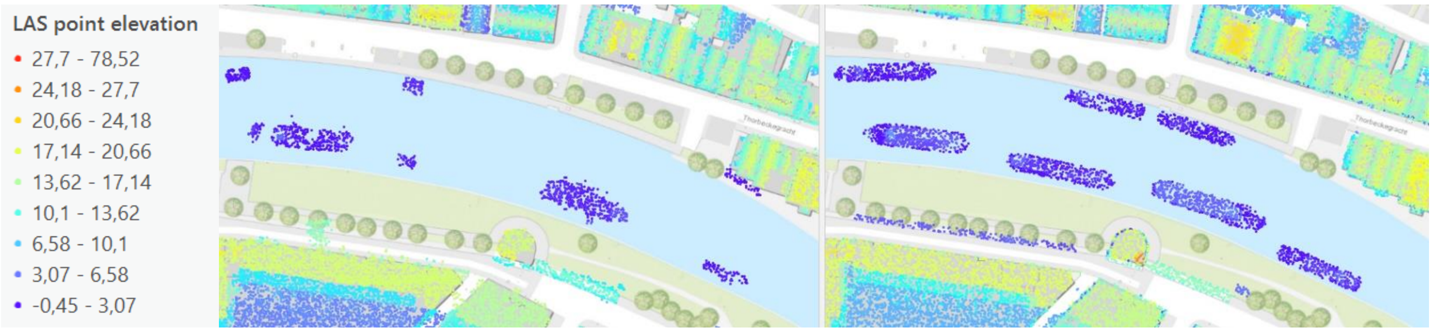

Figure 18. False-negative from LAS thinning result from DIM (left) and LiDAR (right) point cloud. Boat detected as building.

4.1.3. Point cloud registration

Point cloud registration is done based on the ICP algorithm, as explained in Section 3.3.4. After both point clouds were registered, the differences were analyzed and detected by calculating the point to point distances for x, y, z component. The LiDAR point cloud has irregular points, and the DIM point cloud has regular points, so it is incomparable in the x and y component. Therefore to detect the changes in urban objects, we focused on the z value. In Figure 19 and Table 9. Result point to point distance calculation of two dataset., we presented the mean distance (μ) and the standard deviation (σ) from point to point distance with color codes using meters as the unit. The source point is the DIM point cloud, and the reference point is the LiDAR point cloud. The red and blue color represents source points that have a higher distance to the reference point. White color represents the source point that closes to 0 or overlap.

In Figure 19 c, there is a clear difference between the two datasets, also confirmed by the standard deviation in Table 9. This difference might be due to the different acquisition time. These unmatched areas furthermore, were checked visually using Cyclomedia and Google Maps (Table 10). From those resources, we noticed there are four unmatched areas because the building shapes have been changed. To check the positional accuracy of the registration process of the two datasets, those unmatched areas were removed, and the rest of the point clouds were re-registered and recalculated. From the data represents in Table 9, we show that the standard deviation is reduced drastically.

In the end, to create the most current point cloud dataset and to achieve the aim of the temporal quality, we used the DIM point clouds in those unmatched areas.

Table 9. Result point to point distance calculation of two dataset.

Component	With unmatched area		Unmatched area removed	
	Mean distance (μ)	Standard deviation (σ)	Mean distance (μ)	Standard deviation (σ)
x	0.059m	2.800m	-0.017m	1.137m
y	0.047m	2.430m	-0.079m	1.041m
z	0.082m	1.914m	-0.046m	0.788m

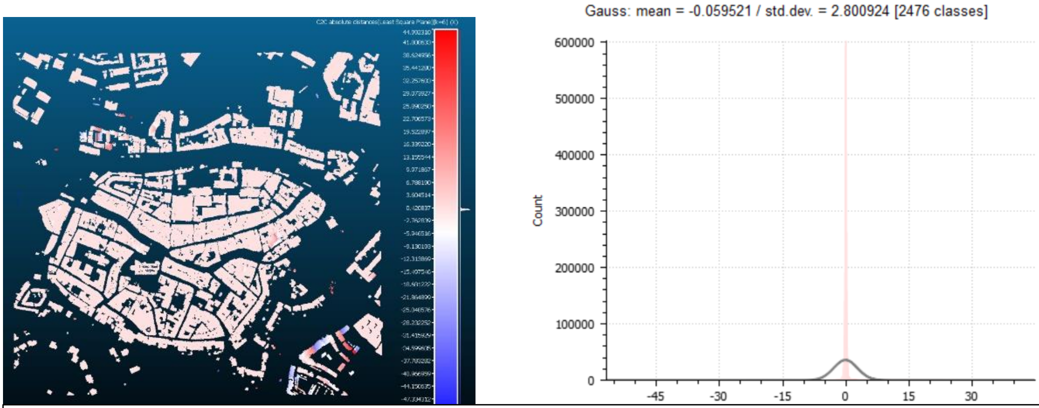

(a) X component

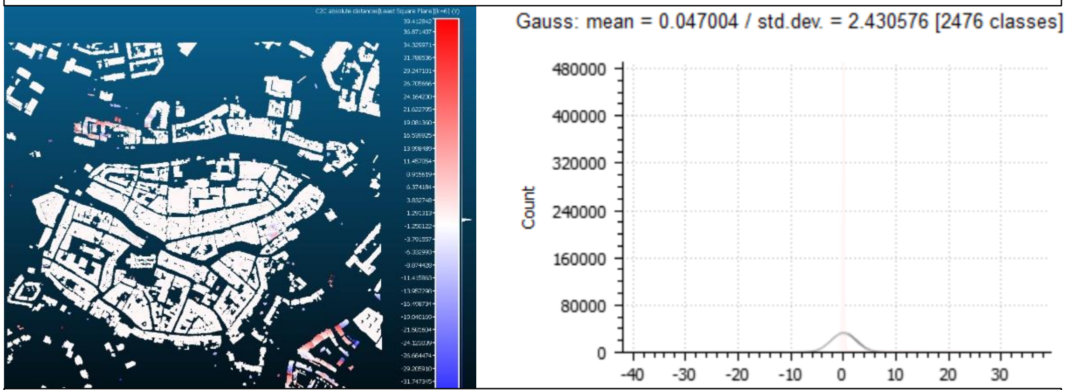

(b) Y component

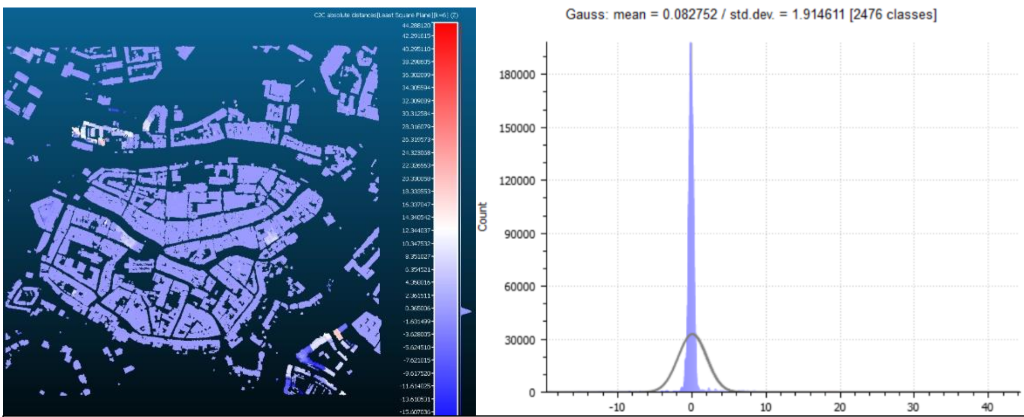

(c) Z component

Figure 19. Point to point distance calculation in x (top), y (middle) and z (bottom) component.

Table 10. Unmatched areas from two-point cloud datasets compared with Cyclomedia and Google Maps.

DIM	LiDAR	Cyclomedia	Google Maps
1. Area: Papenstraat 9			
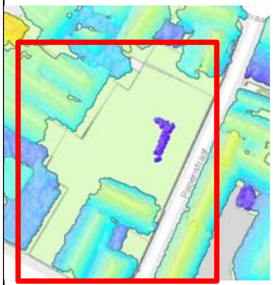 (2019)	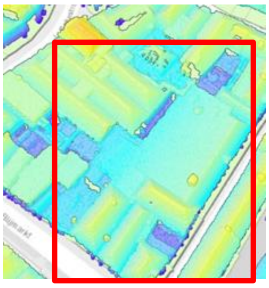 (2016)	 (2019)	 (2018)
2. Area: Friesewal 49-53			
 (2019)	 (2016)	 (2018)  (2020)	 (2020)
3. Area: Spoelstraat 18			
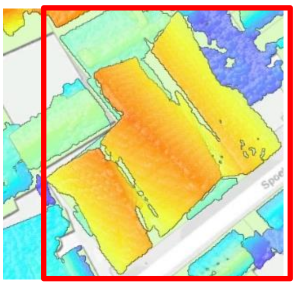 (2019)	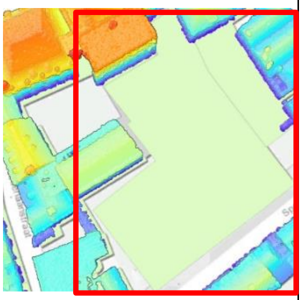 (2016)	 (2018)	 (2020)
4. Area: Voorstraat (lower boundary) and Melkmarkt (upper boundary)			

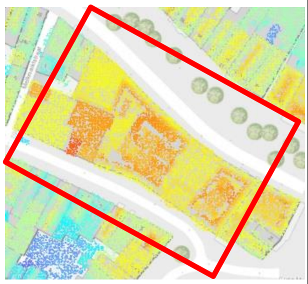 (2019)	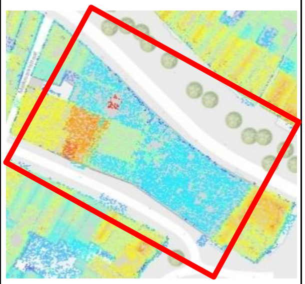 (2016)	 (2016)  (2019)	N/A

4.2. Result of the 3D models

The final result of the generated 3D models is shown in Figure 20. From the process elaborated in section 3.4, we generated 48 buildings from the study area. The semi-automatic method successfully generated different primitive roof types, such as cross hipped, mansard and hip valley (Figure 21).

Figure 20. The result of the generated 3D models, 48 buildings are generated from the study area.

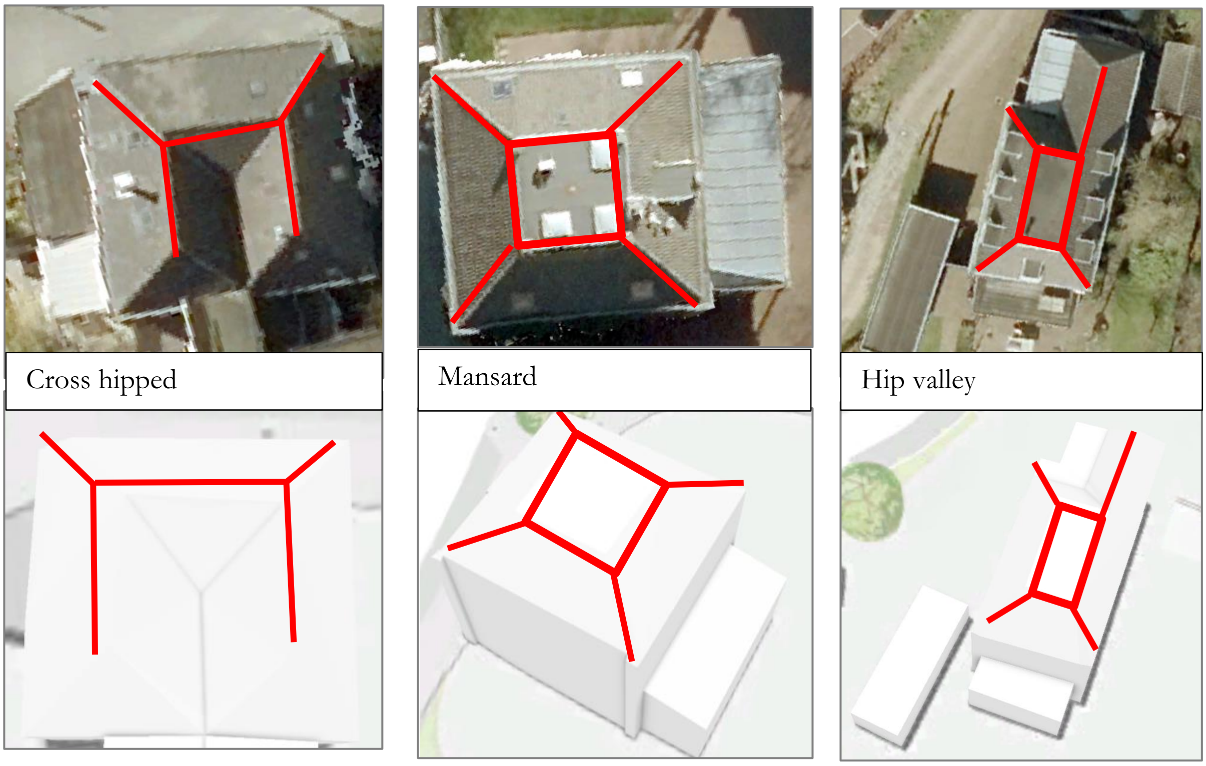

Figure 21. Different types of roofs are generated, cross hipped, mansard and hip valley.

In the case of solar photovoltaic potential analysis, modeling the roof type is important because roof types determine areas available, which also determine the amount of solar panel can be installed and the energy can be harvested. Challenges that need to be better addressed are related to the deviation position between the building footprints and the rooflines. Due to deviations between the input data, it is challenging to implement a fully automatic method. In this case, we set the building footprints obtained by BAG as a benchmark.

4.3. Result of solar photovoltaic potential calculations

We converted the 3D models of 48 buildings to DSM because the main input of the Area Solar Radiation tool in ArcGIS is DSM. As part of the experiment, we converted the 3D model with different pixel sizes, 0.2m and 0.5m pixel resolution. (Figure 22a and Figure 22b). As explained in Section 3.5, we also generated another DSM with the same pixel size directly from the integrated point cloud (Figure 22c and Figure 22d). These DSMs were used as input for solar radiation analysis and the results are presented in Appendix 3. Figure 22 presents the result from one building.

Following the explanation in section 2.3.1, we ran the solar radiation analysis in two steps: calculate the physical potential and calculate the geographic potential with Area Solar Radiation tool from ArcGIS. The tool produced a raster layer where each pixel value is the amount of solar radiation in units of Wh/m^2. The physical potential calculated the solar irradiation on all roofs for the whole year of 2019 with 0.5 as hour interval. The hour interval determines the tool to compute the amount of solar radiation once every half hour for each day; otherwise, the tool will calculate an aggregated solar radiation for each day. The criteria applied in the geographic potential were derived from the findings from the semi-structured interviews. We noticed differences in determining the criteria, as explained in section 4.4.1. Therefore we adopted one of the criteria that took a similar geographic area as our study area. Table 11 described the criteria.

Table 11. Criteria applied to estimate the solar potential.

Criteria	
Feasible slope	38 degrees
The minimum threshold for irradiation per year	600 kWh/m²
Feasible roof orientation	South facing

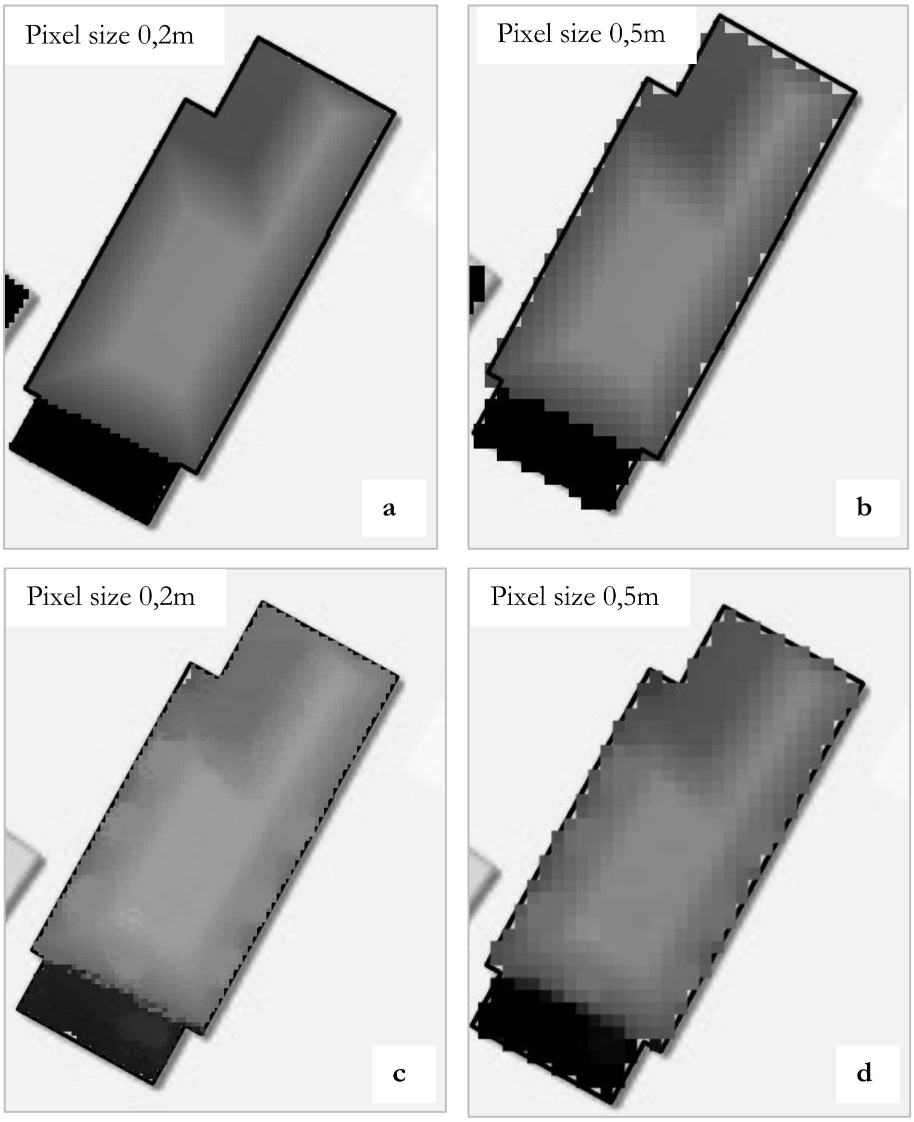

Figure 22. Comparison between DSM. Picture (a) and (b) are generated from the conversion of a 3D model. Picture (c) and (d) were generated directly from registered point clouds.

Figure 23 represents the result of physical potential from one building (see Appendix 4 for the result from all buildings in the study area). It can be seen from the experiment, that the result of solar radiation analysis carried with our methodology (Figure 23a and Figure 23b) produces a much smoother result compare with the result carried with DSM (Figure 23c and Figure 23d). With the presented 3D model technique, roof details such as dormers to quantify available surface areas were hard to be obtained. By using the converted 3D model as input data for solar radiation, the analysis could avoid data gaps and noise that likely happened if using DSM. The result of the integrated point cloud demonstrated that it is sufficient to produce a 0.2m pixel resolution DSM.

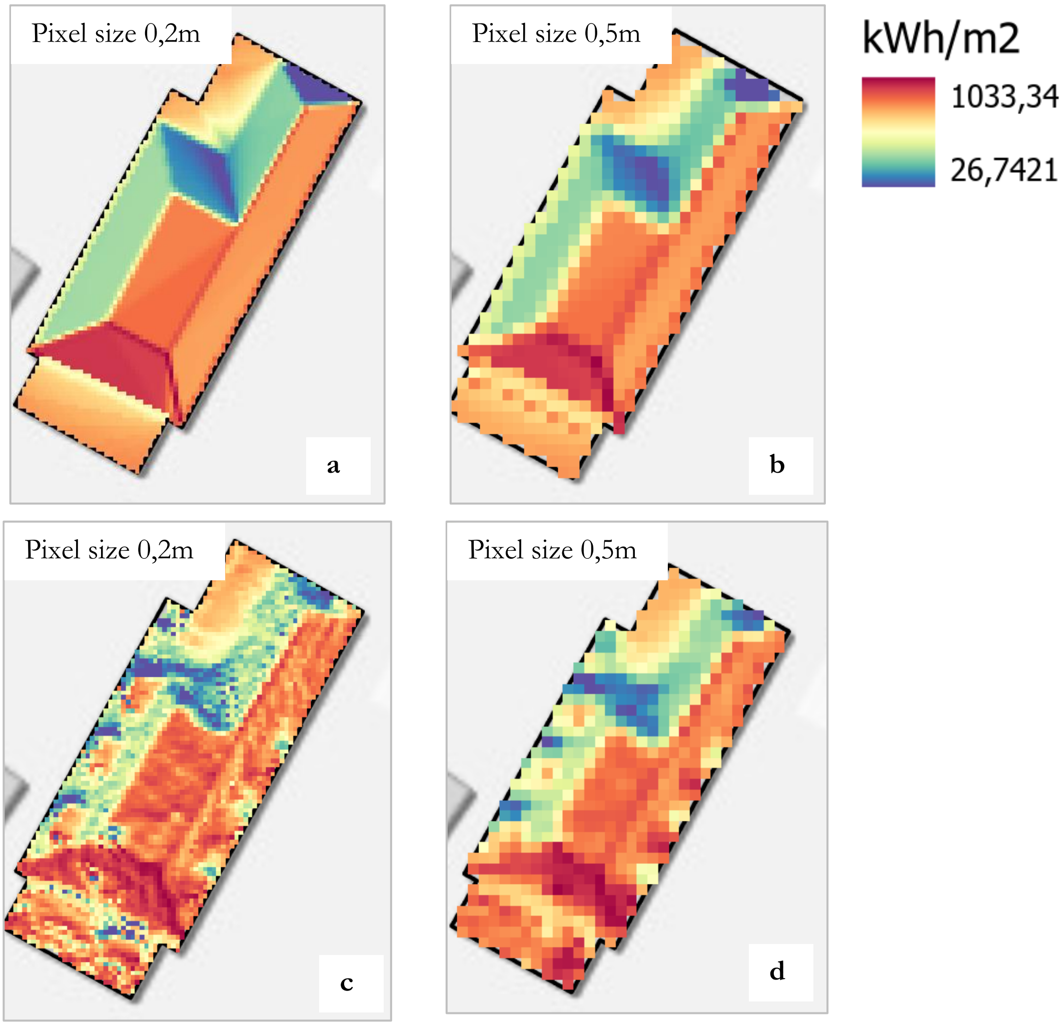

Figure 23. The comparison between the result of solar radiation analysis. The input data for (a) and (b) are the converted 3D model. The input data for the picture (c) and (d) are DSM generated from the integrated point cloud.

From this result, we applied the criteria from Table 11 to calculate the geographic potential. Firstly, the roof slope is calculated to determine the incline of the roof—the slope calculation resulting in value ranging from 0-90 degrees per pixel. The lighter colors represent lower slopes, and darker colors represent steeper slopes (Figure 24, see Appendix 5 for the result from all buildings in the study area). Afterward, we created the aspect layer to determine the roof orientation (Figure 25). Each pixel contains value represent orientation in degrees, 0 represents absolute north, and 180 represents absolute south. The Netherlands located in the northern hemisphere, therefore roof surfaces facing the north are likely to receive less solar radiation than roof surfaces facing other directions. Thus roof surfaces that facing other directions will receive more solar irradiation.

We started by applying the feasible roof slope criteria. Thus we removed roof surfaces less than or equal to 38 degrees. Next, we applied the minimum threshold criteria; thus, roof surfaces with low solar radiation below 600kWh/m^2 were removed. From the result of this step, most roof surfaces facing other orientations except the south were likely removed. However, there are still some roof surfaces facing north remain, so we removed these roof surfaces. After the criteria are applied, we obtained the potential areas for solar photovoltaic installation shown in Figure 26.

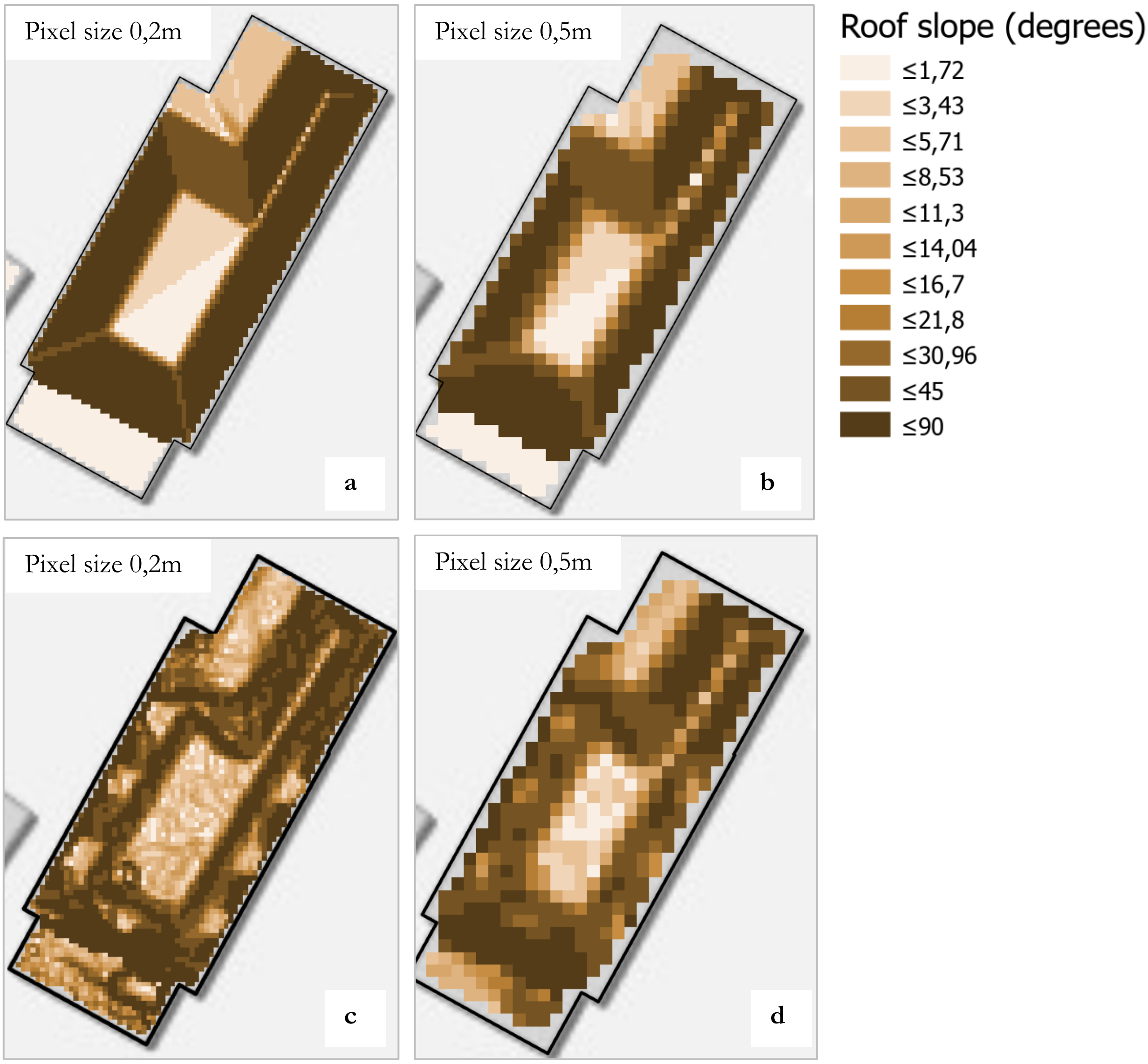

Figure 24. The comparison result of roof slope calculation from one building. The input data for (a) and (b) is the converted 3D model and the input data for (c) and (d) is DSM from the integrated point cloud. To see the result from all buildings, see Appendix 5.

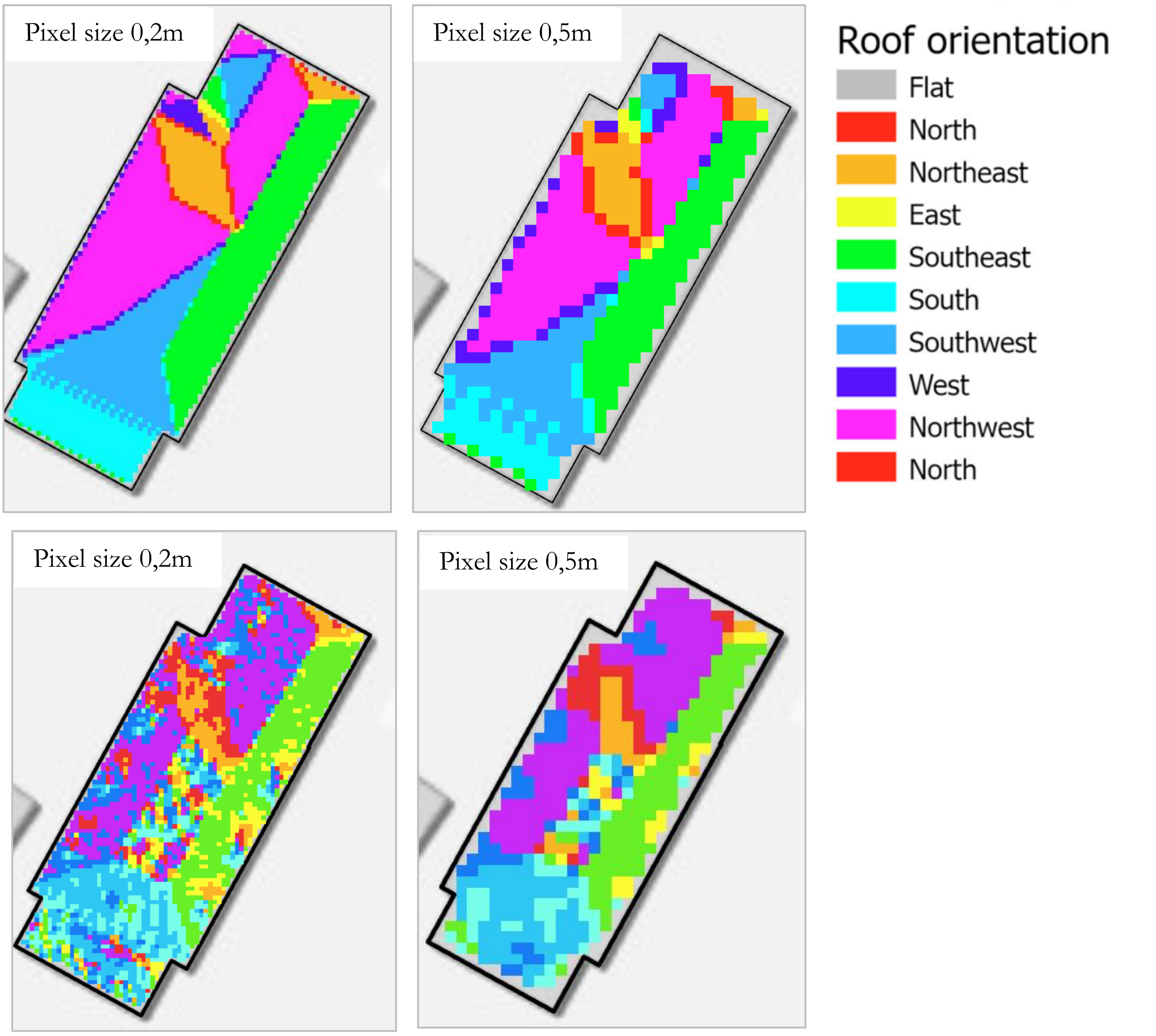

Figure 25. The comparison result of roof orientation calculation from one building. The input data for (a) and (b) is the converted 3D model and the input data for (c) and (d) is DSM from the integrated point cloud. To see the result from all buildings, see Appendix 6.

The output of the calculation is still meaningless because it shows solar radiation values in each pixel. Therefore, we aggregated the pixels to know how much radiation each building could harvest. To calculate the total amount of solar radiation received per year by each building's usable area, we multiplied the suitable areas by the average solar radiation; the result is presented in unit MWh for the year 2019. From the 48 buildings used as input data, only 45 buildings meet the criteria. The amount of energy to harvest differs among the four input datasets (Table 12). The differences for each building are relatively small, shown in Figure 26.

Table 12. Energy to harvest for one building in a year corresponds to Figure 25.

Input data	Area (m^2)	Average solar radiation (kWh/m^2)	Energy to harvest (MWh)
Converted 3D model 0.2m pixel resolution	46.72	817.351	38.19
Converted 3D model 0.5m pixel resolution	38	810.884	30.81
DSM from the integrated point cloud 0.2m pixel resolution	42.96	793.315	34.08

DSM from the integrated point cloud 0.5m pixel resolution	37	802.191	29.68

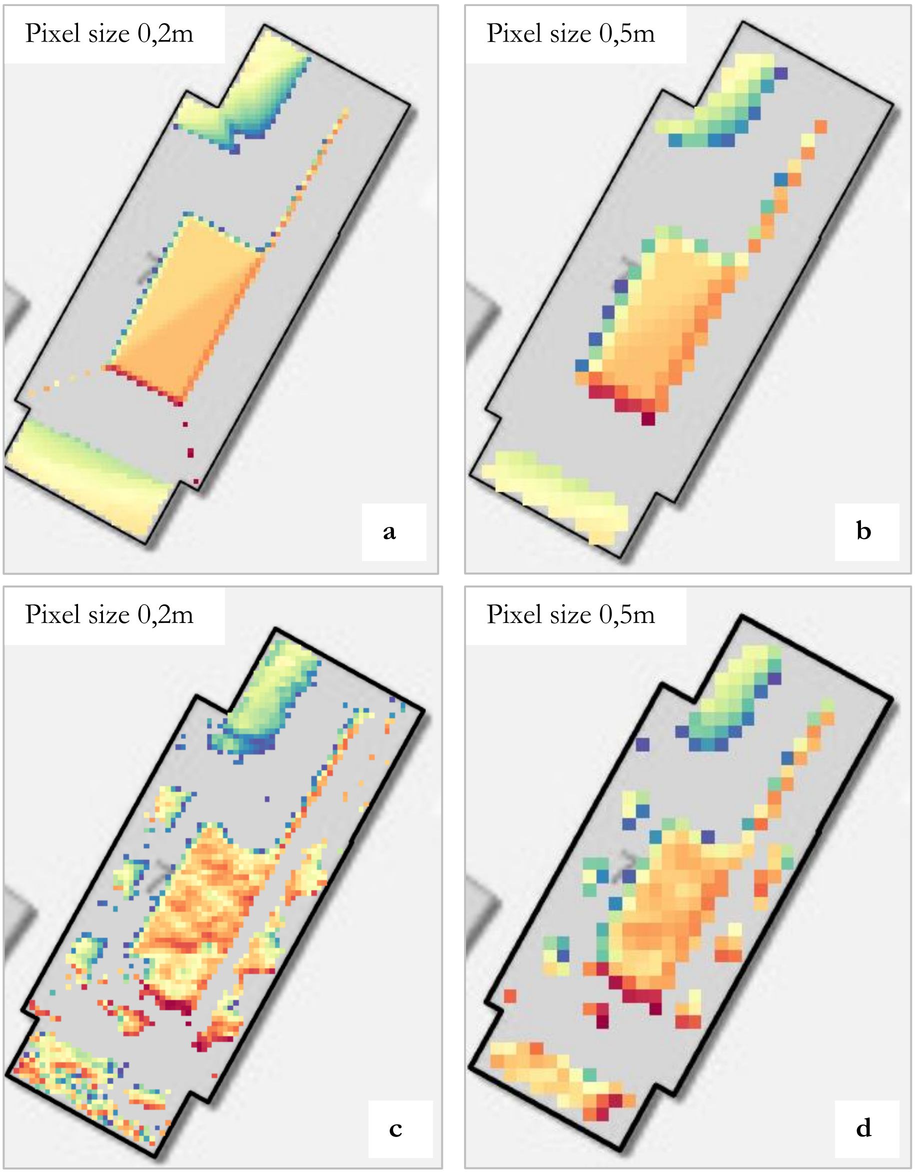

Figure 26. Comparison result from one building after the criteria are applied, resulting in the potential roof surfaces. The input data for (a) and (b) is the converted 3D model and the input data for (c) and (d) is DSM from the integrated point cloud. To see the result from all buildings, see Appendix 7.

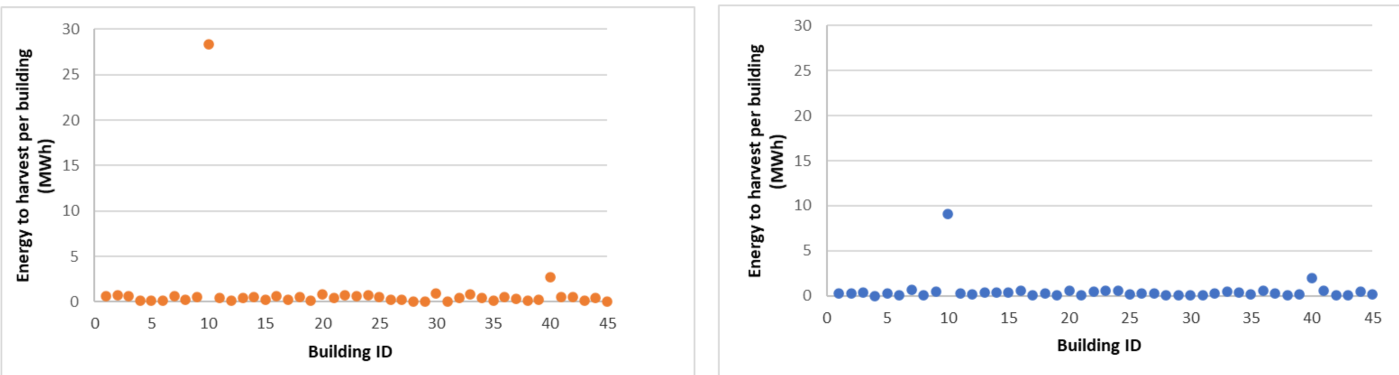

Figure 27. The difference in the amount of energy to harvest for each building in a year.

Table 13. Energy to harvest for the total 45 buildings dataset in a year.

Input data	Energy to harvest (MWh)
Converted 3D model 0.2m pixel resolution	907.121
Converted 3D model 0.5m pixel resolution	939.138
DSM from the integrated point cloud 0.2m pixel resolution	693.938
DSM from the integrated point cloud 0.5m pixel resolution	918.304

On the converted 3D model, details are generalized and noises are removed as opposed to a DSM from the integrated point cloud, where these are shown. Figure 26 demonstrates the difference, the roof details on the roof segment were mostly removed when using the converted 3D model (Figure 26a) while it remains when using DSM from the integrated point cloud (Figure 26c) and is extracted as potential areas. These reasons could explain the difference when estimating solar radiation potential. Integrating more datasets and generalization in generating 3D models could introduce unidentified errors, which might add to the differences found.

Figure 27 shows the difference in the amount of energy to harvest for each building in a year. Two outliers are referring to a big difference in the calculation when using a converted 3D model and DSM from the integrated point cloud as input data, noticed from these charts. When these two outliers are checked closely and compared with aerial imagery and the point cloud used, we recognized that the top surface of the building contains objects that are generalized in the converted 3D model (Table 14). From the aerial imagery, we noticed that the roof structure of building number 10 is complicated and hard to define the height jump and roof edge from this building. While for building number 40, the roof surface is planar with an object resemblance to a wall in between. From these two cases, manual digitization for rooflines might be confusing because the objects are vague to consider as height jump and roof edge. These findings might help us to understand that the semi-automatic method used in this study is needed an improvement to avoid variation in the result of the solar photovoltaic analysis.

However, the ground truth needed to assess the outcome of this calculation process is not available, limiting the options to prove the result, whether it is close to reality or not.

Table 14. Outliers detected between input datasets. Comparison between aerial imagery, input data models, and potential roof surfaces.

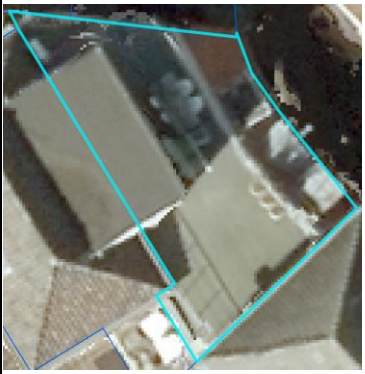 Aerial imagery of the building number 10.	 Aerial imagery of the building number 40.
Converted 3D model with 0.2m pixel resolution.	

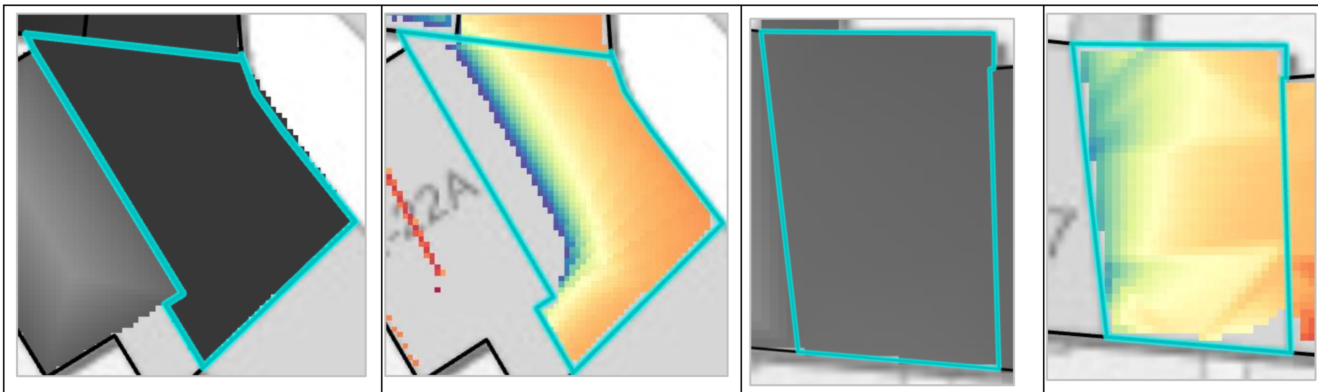

Converted 3D model with 0.5m pixel resolution

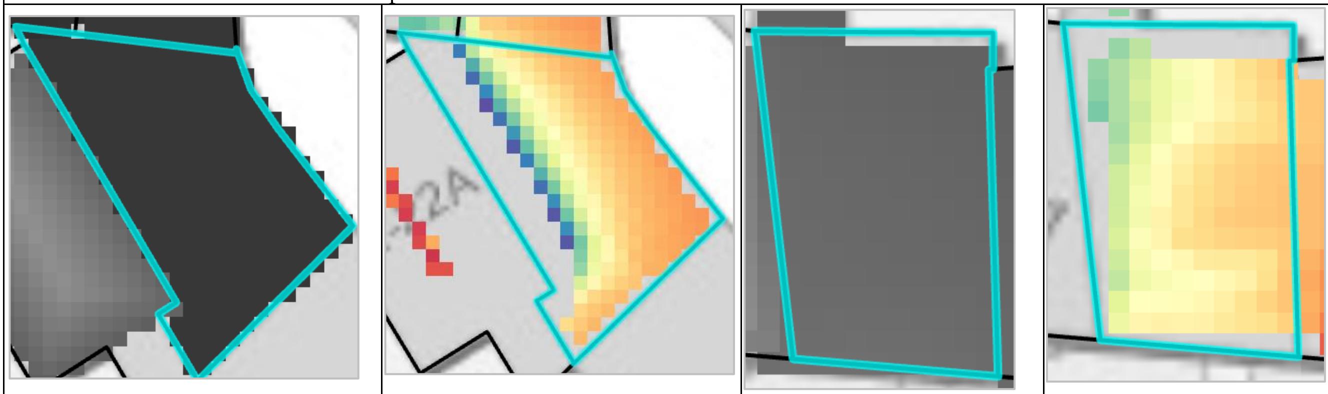

DSM with 0.2m pixel resolution

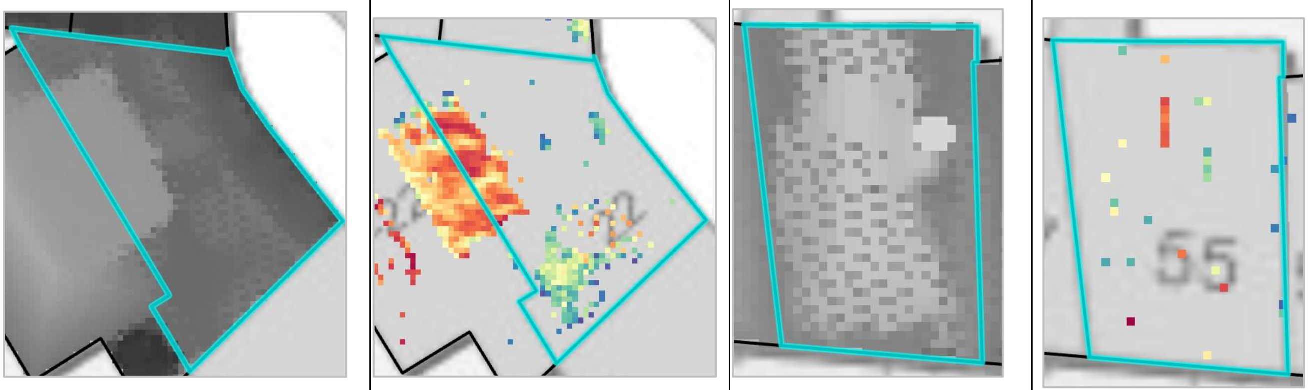

DSM with 0.5m pixel resolution

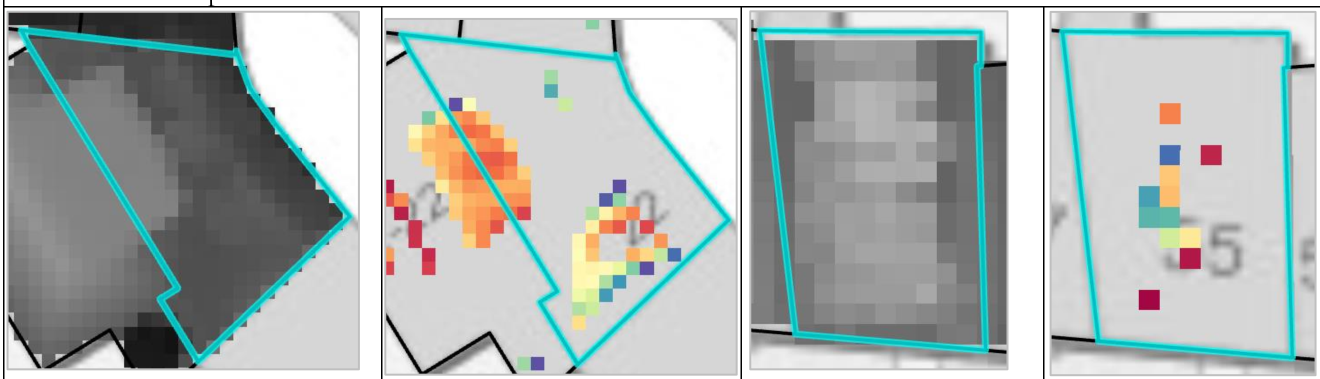

4.4. Result and implications of semi-structured interview

This section analyses the results of the interviews conducted among representatives of four different backgrounds (section 3.6.1). The interviewees are experts from diverse backgrounds, municipality (Interviewee 1), solar analysis provider (Interviewee 2), land-mapping agency (Interviewee 3) and academia (Interviewee 4). These professionals represent different knowledge areas involved in the solar photovoltaic analysis. The results are described in section **Fout! Verwijzingsbron niet gevonden.**– 4.4.3. Section **Fout! Verwijzingsbron niet gevonden.** elaborates the required information related to input data to estimate solar photovoltaic potential. Section 4.4.2 analyses the compliance and shortcomings of the current 3D data. Section 4.4.3 explains the topics that aimed at identifying the need for standard 3D input data for solar photovoltaic analyses.

4.4.1. Required information for solar photovoltaic potential estimation

The four experts were asked to give their point of view about the **general factors required to estimate the solar photovoltaic potential.** The four interviewees explicitly stated the general factors used to calculate the estimation of solar photovoltaic potential are (Figure 28):

a. Information about roof: slope, type, and orientation;
b. Shadow casting from surrounded buildings and trees.

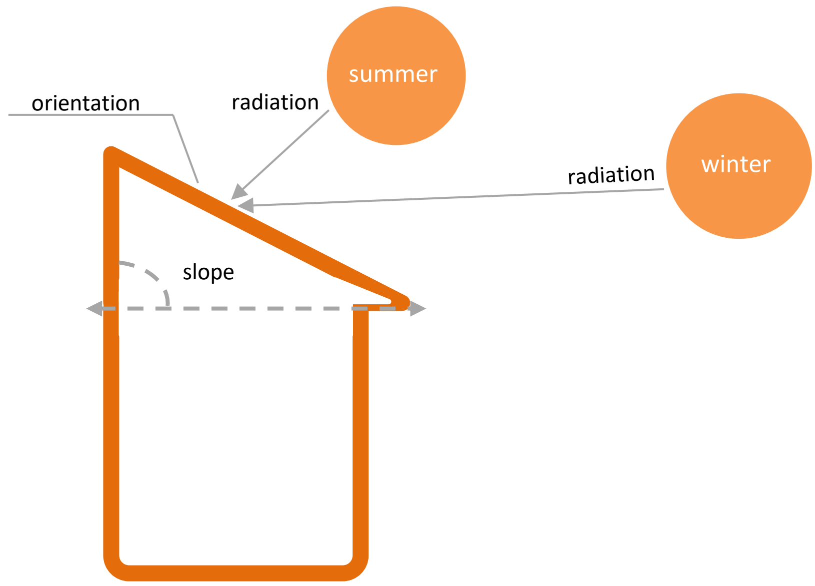

Figure 28. The general factors used to calculate the estimation of solar photovoltaic potential.

Interviewee 1, stressed that in the municipality of Zwolle, there **are two extra regulations** applied. First, solar photovoltaic panels are not allowed to be installed on historical buildings' roofs and special roof shapes. Second is the line of sight regulation for the city center of Zwolle; it is not allowed to install solar photovoltaic panels if:

a. the solar photovoltaic panel is visible from Zwolle four points of interest (Peperbus, Museum de Fundatie, the Town Hall, and the Sassenpoort;
b. the solar photovoltaic panel is visible from publicly accessible areas.

However, all four interviewees underlined that the solar photovoltaic potential areas are reduced when factors such as mentioned above restrict the suitability analysis. Other factors are added by Interview 2 about minimal roof surface area also by Interviewee 3 about the minimum threshold for production of solar energy for each building per year and the optimal roof slope. According to both interviews, these two factors are related to the payback period, which founded important for citizens and municipalities. The importance of these factors is also acknowledged by the research from Paardekooper (2015) and Peronato et al. (2016). However, Paardekooper (2015) and Peronato et al. (2016). Yet, inconsistencies were found for determining the optimal roof slope and threshold for the production of solar energy for each building per year (Table

15. The threshold applied for suitability analysis of solar photovoltaic.. We assumed that this finding might be the cause of the variation of the result of the solar photovoltaic potential.

Table 15. The threshold applied for suitability analysis of solar photovoltaic.

Source	Study area	Slope	Orientation	The minimum threshold for production of solar energy for each building per year (kWh/m2/year)
Broersen et al. (2018)	The Netherlands	-	South	690
Prieto, Izkara, & Usobiaga (2019)	Vitoria-Gasteiz, Spain	38	South	800
Biljecki, Heuvelink, Ledoux, & Stoter (2015)	Delft, the Netherlands	40	-	850
Peronato et al. (2016)	Neuchâtel, Switzerland	-	South	Tested in various threshold: 400 - 1200
Peronato et al. (2018)	City of Geneva	-	South	1000
van Sark (2014)	The Netherlands	40	South	875
Paardekooper (2015)	Amsterdam, the Netherlands	33	South	969
Kausika et al. (2015)	Apeldoorn, the Netherlands	38	South	600
Zonatlas	The Netherlands	40	South	-

4.4.2. Compliance and shortcomings from the current 3D data

Each expert was asked at the beginning of the interview to indicate their knowledge on the main topics of the interview:

1. Knowledge of 3D data and GIS analysis;
2. Quality in the current 3D data available (definition of quality explained in section (section 2.1.3);

The results showed that all interviewees are familiar with 3D data and GIS analysis, although two out of four interviewees are not using it on a daily basis. Their knowledge regarding the quality of the current 3D data available, i.e., AHN, is valuable because it gives insight about the perspectives of the users and to identify the needs from the users on the 3D data. To be specific, 3D data available that being discussed were AHN.

The interviewees mainly mentioned **temporality and spatial accuracy as the two important features of 3D data quality**. Interviewee 2 said that the current height information available does not satisfy them in terms of temporal acquisition time, which was confirmed by Interviewee 3 and Interviewee 4. Interviewee 2 expects from the data providers to have more recent height information and higher resolution dataset. A higher resolution data will be useful to allow for more detailed calculations of the solar photovoltaic potential per roof for assessing the economic feasibility, stressed by Interview 2. However, Interview 2 did not take the initiative to acquire extra data, i.e. point clouds, themselves because such data is too expensive and costs extra work. Interviewee 3 explained that **with the help of aerial imagery that is yearly collected, they could derive a point cloud from aerial imagery; such a dataset could compensate the temporal quality, completeness and spatial resolution**. However, Interviewee 3 said that adding an additional dataset might introduce a new error.

Interviewee 4 specifically mention **to detect objects on top of the roof image recognition techniques, for example, deep learning.** For instance, by adopting the technique to detect damage on the road (Angulo, Vega-Fernández, Aguilar-Lobo, Natraj, & Ochoa-Ruiz, 2019) and combined with rooftop segmentation (Collier et al., 2019).

4.4.3. Purpose of a standardized model for solar photovoltaic analysis

Interviewees were asked their opinion about a standardized model for solar photovoltaic and what the general requirements would be of use in the case in terms of (1) the most important quality in datasets and (2) data dimensionality. The opinions of the four experts about requirements for a standardized model for estimate the solar photovoltaic potential are:

1. **There is no consensus among the interviewees concerning a standardized model for solar photovoltaic potential**. Interviewee 3 stressed the importance of a good temporal resolution that allows having an up-to-date dataset.

2. **The most important quality in datasets is temporal and spatial accuracy**, which repeatedly mentioned by the four interviewees, as elaborated in section 4.4.2. In terms of an object that could be detected, both interviewees 1 and 2 mentioned particularly *"information about roof"* and *"windows, chimneys, and dormer"* respectively.

   According to Wong & Ellul (2012), current desktop assessment is considered crude and mainly for preliminary investigation, whereas on-site assessment is still placed as a compulsory step. Nouvel, Schulte, Eicker, Pietruschka, & Coors (2013) also acknowledged that having information about roof windows is important. Although nowadays highly-detailed data is adequate to detect roof and windows, the on-site survey is also used to check roof material, because it is not detectable from LiDAR nor DIM point clouds, as stressed to Interviewee 3. Interviewee 2 stated that providing a detailed assessment for preliminary calculation would make the prospective consumer uncertain, *"adding too much detail could start a discussion in the mind of the consumer"*. Therefore mentioned by Interviewee 2, a detailed calculation is only used if the customer asks.

3. The literature review (section 2.3.3) showed that the input data for calculating solar photovoltaic potential are based on 2.5D or 3D data because it contains information about elevation, orientation, the slope of rooftops and shadows from surrounding features. Stated by interviewee 3 and 4, that **"to calculate solar photovoltaic potential on the roof, the 2.5D model is enough and a 3D model is required to calculate solar photovoltaic potential of the façade"**. This statement is in line with the literature findings from Machete (2016) and Peronato et al., (2018). However, mentioned by Interviewee 3 there is a demand from the Netherlands to invest in a high-quality 3D model.

4.5. Result from the focus group discussion

The focus group discussion was held through an online session. The perceived quality of the 3D model of the six participants was measured using qualitative indicators that include fit-for-purpose, general validation statements, and data integration. The session was started with an introduction about the research with presentation and video, followed by filling the questionnaire because of the online situation (see Appendix for the questions and link to the video). The perception was measured on a scale of 1 (strongly agree) to 5 (strongly disagree), or no response, followed by several open questions. At the end of the session, we presented the outcome of the questionnaire to facilitate discussion between participants. The participants are six experts in 3D modeling, point cloud and are familiar with the solar photovoltaic application. The results of the focus group discussion are described in section 4.5.1-4.5.4. Section 4.5.1 presents the discussion relate to fit-for-purpose. Section 4.5.2 elaborates the findings of general statements, followed by section 4.5.3 elaborates the discussion about data integration. In the end, section 4.5.4 summarized the main findings from the focus group discussion.

4.5.1. Fit-for-purpose

To evaluate the fit-for-purpose of the 3D model for solar photovoltaic potential analysis, six participants were asked to give their perception of the 3D model quality. We obtained various responses regarding the need to use a 3D model as an input for solar photovoltaic analysis instead of using a DSM raster (2.5D). The response from Participant 3 implies uncertainty by saying, "*I think I'm not sure which one is better and maybe there is no really a distinction between them in* [terms] *which one is the best. But it takes a lot of time to create a 3D model and there is always generalization (from the reality)"*, while Participant 4 disagreed to the statement *"it is not necessary to have the 3D buildings, it can also be done with a DSM however it* [using 3D model] *can be useful and the result looks clearer and less confusion"*.

During the discussion, participants were asked to perceive the effectiveness of the 3D models in providing the required information and the sufficiency for solar photovoltaic analysis. The participants were also asked to assess the effect of pixel resolution for solar photovoltaic analysis on the result. Participant 1 observed that the effect of using 0.2m pixel resolution able to detect roof details than using 0.5m pixel resolution, which is useful for solar photovoltaic analysis. According to most participants, the presented 3D models effectively and sufficiently provides the required information. During the discussion, Participant 2 explained that the 3D models lose some information about the roof details because of the generalization process compare with DSM, "*On the one hand I said that the 3D is so much cleaner that it gives you* [a] *quicker insight. On the other hand, it got so many things it might missed. I'm not sure whether you should use that approach as a source for solar photovoltaic analysis"*. Although, according to another participant, the presented converted 3D models can reduce mistakes caused by data gaps and noise that is likely to happen in a DSMParticipant 3 answered that it is difficult to assess which dataset is better using a survey and discussion the way this session is conducted. As Participant 3 said, *"I think it is very difficult to answer that question because the results are just a visualization of the data"*.

4.5.2. General validation statements

The second section asked the participants to give their suggestions about the possibility of using the 3D models for other applications. All participants agreed that the 3D models could be adapted for other applications, i.e., sound analysis, change detection, and visualization. The participants were asked to list the improvement needed and the major benefits of the 3D models. Two out of six participants listed improvements regarding roof details, i.e., chimney, dormers and windows. Participant 4 suggested having a combination of the 3D models and image processing to recognize dormers, roof windows and chimney for solar photovoltaic analysis. It is interesting to note that this method was also mentioned during the semi-structured by Interviewee 4. Regarding the major benefits of the 3D models, Participant 2 said, "*it looks a lot nicer and people like that, they don't understand a chaotic image. Next to that, there are many other fields where this data could be used instead of solar radiation, there is a big wish for LoD 2.0 in the Netherlands for different reasons, sound calculations is an example"*.

4.5.3. Data integration

Emerged from the semi-structured interview, the four experts from the semi-structured interview found the important features of 3D data quality is the temporality and density. By integrating the LiDAR point cloud and DIM point cloud, temporal quality and the point density of the existing LiDAR point cloud could be improved. To evaluate the result of the integrated point cloud (refer to section 3.3 and section 4.1), we posed four questions regarding the improvement in temporal quality, data completeness and spatial accuracy. Due to the internet connection problem, Participant 6 was unable to participate and answered the questions from this section. Therefore instead of having six answers, we had five answers.

All participants agree that the presented method to integrate both point cloud datasets improves the data completeness. Participant 5 said that this method is suitable to take *'the best of both worlds'*. Regarding the statement "The presented method improves the temporal quality", a variety of perspectives were expressed. Three out of five participants answered with 'agree' and two participants answered with 'neither agree nor disagree' and 'disagree'. During the discussion, the uncertainties found in answers were explained, the two participants think that although there might be an improvement by adding a new dataset (DIM point cloud) to substitute the changing area, it could introduce another error as well. Therefore, it makes the two participants doubting to give the proper answer. This view was echoed by the three participants who are answered 'agree' as well. This explains the fourth question related to an improvement in spatial accuracy; most of the participants answered *no response*.

4.5.4. Findings from the focus group discussion

In summary, these results show that the participants of the group discussion found that the generated 3D models are effective and sufficiently provides the required information for solar photovoltaic potential analysis. Some felt that the generated 3D models lose detailed information. However, when the results of solar radiation analyses are being compared, they noticed that using the converted 3D models could avoid data gaps and noise caused by DSM. Within the focus group discussion, most participants agree that using 0.2m is more useful than using 0.5m as pixel resolution for solar photovoltaic potential analysis. However, uncertainties are shown from the answers of the participants regarding data improvement in temporal quality and spatial accuracy. Figure 29 illustrates the findings from focus group discussion following the dimensions for content analysis; green color represents the dimensions achieved, yellow color represents the dimensions that are uncertain and red color represents the dimensions that are not achieved.

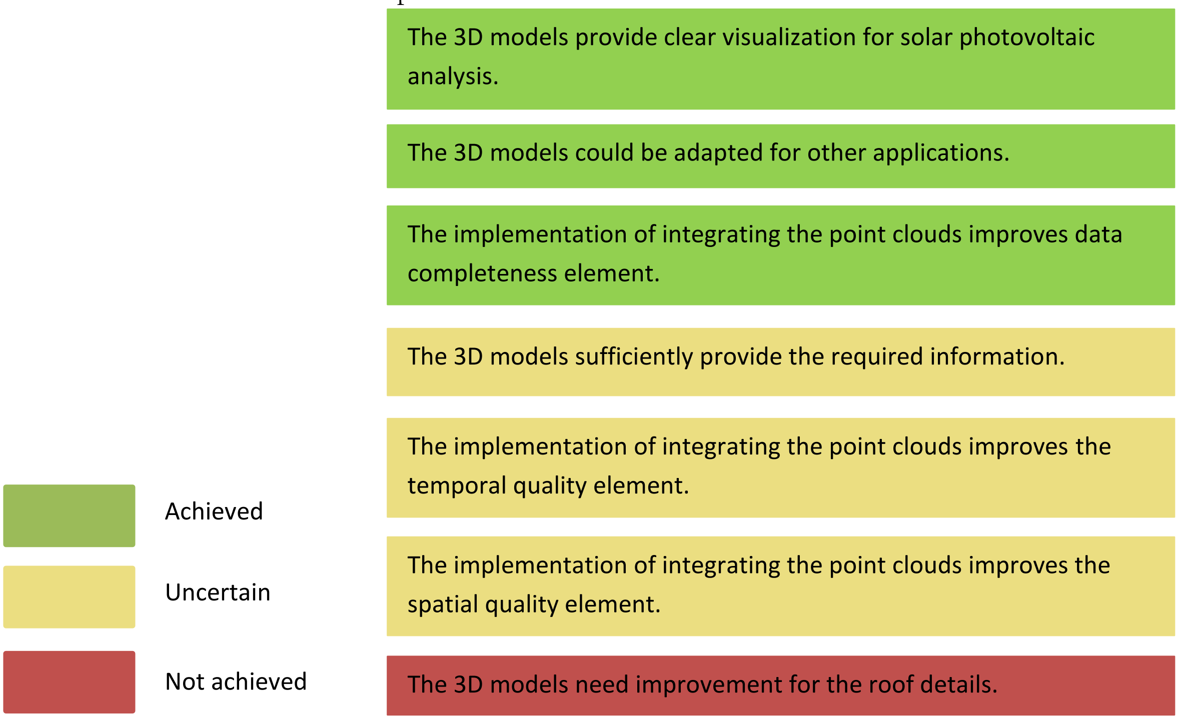

Figure 29. Findings from focus group discussion.

During the discussion, one participant says, *'I always noticed that* [using 3D model] *does really has to do with people just think it's nicer and they understand the data better. We often have a discussion, like, why do people want LOD 2 buildings, you know, or even more. And often the answer is that people, they like the reality and so they don't want blocks, they want* [the building] *as, as it is in reality, they don't like, they don't understand data that look chaotic. They like to* [see] *3D data'*. This statement reveals a hidden benefit and perception from users of using 3D model that is in line with the literature review (see section 2.1.4). Therefore two conclusions were made, the proposed method is fit for the purpose with several improvements and we conclude the solar photovoltaic analysis can benefit from using a 3D model as the input data and as the visualization for the output.

4.6. Summary

This chapter presented and described the results for pre-processing 3D data, 3D model generation process, solar photovoltaic potential, semi-structured interviews and focus group discussion. The LiDAR point cloud and DIM point cloud were integrated and used as input for the 3D models. The methodology applied generated 48 buildings as input data for calculating the solar photovoltaic potential. Next to that, we generated DSM from the integrated point cloud to compare the usability of the 3D model and effect from using finer pixel resolution to the solar photovoltaic analysis. From the 48 buildings used as input data, only 45 buildings meet the criteria.

From the result of the experiment, the calculation results of the solar photovoltaic potential are different when using 3D model as input data. The generalization of the roof details and the removed noises when using 3D model could explain the difference when estimating solar radiation potential.

Findings emerging from the semi-structured interview show that the temporal quality of the currently available 3D data does not satisfy the users. Revealed from the focus group discussion, the method to integrate the LiDAR point cloud and DIM point cloud improve the data completeness and temporal quality element. Two conclusions from the results of the focus group discussion, the proposed method is fit for the purpose with several improvements for the roof details by including i.e. chimney and dormers.; second, the solar photovoltaic analysis can benefit from the 3D model as the input data and as the visualization for the output

5. CONCLUSION AND RECOMMENDATION

This chapter provides reflections on the research objectives of the study. Conclusions and recommendations for future research are also presented.

5.1. Reflection on the research objectives

This study aimed to explore the possibility of integrating two different point cloud to produce a unified dataset that can suit many applications. The suitability of this dataset is tested through simulation on a use case of estimating solar photovoltaic analysis. A discrepancy has been found between the quality of the current datasets and the needs of the users. We found that the temporal quality of the available LiDAR point clouds does not comply with the needs of the users. The integration of LiDAR point clouds and point clouds derived from the dense image matching technique were proved to produce a unified dataset that complies to the temporal quality.

Sub objective 1: To investigate the characteristics of the input data.
In this research, we used the LiDAR point cloud and a DIM point cloud. The integration from these two datasets is a powerful method to generate 3D models. Our study found that the main problem when performing data integration is to correctly and accurately integrate the datasets when those data sets have different accuracy, density and properties.

The foundation to determine the quality of the 3D model is to assess the quality of the input data. Following the six elements of data quality from ISO 19157: 2013 (ISO, 2013), we used completeness, temporal quality, and positional accuracy to determine the quality of the input data. These elements were used because those elements have a significant impact on the geometric aspect of 3D data. The fusion of LiDAR point clouds with DIM point cloud is a popular combination because it could combine the best of both to increase completeness, temporal quality, and positional accuracy, which determines the quality of the input data that covered in this research.

In this study, we used the Iterative Closest Point (ICP) algorithm to register the DIM point cloud to the reference point, the LiDAR point cloud. The principle of this relative positioning algorithm is to find corresponding points between two-point cloud datasets. A major advantage of this relative positioning algorithm is that, it reduces fieldwork to collect ground control features because only one data set, in this case, LiDAR, has to be georeferenced.

Sub objective 2: To prepare unified data that satisfy the user needs for 3D models.
As identified from the result of the semi-structured interview, the majority of participants explicitly stated the similar general information required to calculate the estimation of solar photovoltaic potential. The required information is roof slope, roof type and roof orientation, next to shadow casting from surrounded buildings and trees. Therefore this information is implemented in the 3D model generation.

The interviewees acknowledge during the semi-structured interviews that the currently available height information (LiDAR point cloud-AHN) does not comply with the needs of the users in terms of temporal acquisition time. According to the interviewees, temporality and spatial resolution are the two important elements to determine the quality of 3D data. One interviewee mentioned that adding an additional datasets such as aerial imagery, it could compensate the temporal quality, completeness and spatial resolution. To solve this issue, adopting the DIM point cloud as another source of height information was seen as a possible solution that was explored in this research. The need of the users regarding the quality elements can be compensated by integrating the LiDAR point cloud (current height information) and DIM point cloud to produce a recent height information data (yearly), reduce the data gap due to the acquisition process, and improve positional accuracy.

Sub-objective 3: To develop a 3D model to estimate the potential of a solar photovoltaic installation.
This research used the RANSAC algorithm to develop a 3D model for the study area. The method was chosen based on the existing methodology used at Kadaster. During the trajectory of this research, we explored several methods to generate the 3D model with procedural modeling and footprint partitioning with Douglas-Peucker and region growing algorithm. However, after comparing these methods, the RANSAC algorithm turned out to be more accessible and straightforward to be used in this research than the previously mentioned methods. In this research, the method used to estimate the potential of solar photovoltaic is the Area Solar Radiation tool from ArcGIS. This tool is straightforward and requires a raster as its input data.

From the result of the experiment, the calculation results of the solar photovoltaic potential are different when using converted 3D models as input data. The roof details on the roof segment were generalized and noises were removed, while it remains when using DSM from the integrated point cloud. This could explain the difference when estimating solar radiation potential. From the experiment of comparing different pixel resolution and different models of input data, using 0.2m for pixel resolution is able to detect roof details than using 0.5m.

According to the result of the focus group discussion, the developed 3D model is effective in providing the required information and sufficient for solar photovoltaic analysis. Also, using the 3D model instead of DSM could avoid noise and data gaps. During the focus group discussion, the participants mentioned that the generated 3D model could be adopted in other applications. However, the generated 3D model, according to the result of focus group discussion, needs further improvements for the roof details.

5.2. Conclusions

This study contributes to the investigation of standard 3D input data for solar photovoltaic in the Netherlands. Furthermore, this study successfully explored the opportunity to produce a complete, recent, and positionally accurate point cloud dataset by integrating DIM point cloud and LiDAR. We revealed a hidden benefit and perception from users when using the 3D model, that people prefer to view a representation of reality which 3D can provide for them. Therefore, these findings provide a new understanding that the solar photovoltaic analysis benefits from using the 3D model as the input data and as the visualization for the output.

The presented method allows constructing semi-automatic 3D models from the integrated point clouds, building footprints and rooflines. The 3D model supports the assessment of the solar photovoltaic potential. Further investigation to fully automized the 3D model generation will be valuable to scale up the method and the study area.

From the experiment conducted in Zwolle, the Netherlands, comparing two datasets with two different pixel sizes to see the effect of the finer resolution, the results showed that the finer pixel resolution influences the solar photovoltaic potential analysis. This study provides insights to support the Kadaster in 3D model and solar photovoltaic potential analysis.

5.3. Recommendation

Based on current research, recommendations for future works are listed as follow:

1. Advanced techniques to generate a fully automatic 3D model need to be explored to scale up the method.
2. Automatic rooflines extraction to generate rooflines dataset.
3. Image recognition technology could be utilized to detect objects on top of the roofs as part of the analysis of solar photovoltaic potential.
4. During the trajectory of this research, it is interesting to explore the possibility of detecting urban changes with LiDAR point cloud and DIM point cloud.

5.4. Limitations

While this research tried to provide an integrated view of all aspects, due to a fixed timescale we had to narrow down the scope of this research. In the limited time at Kadaster, we were not able to fully automate the process of generating 3D models. Also, the focus has been on the area of Zwolle. Other areas, like rural, urban or high-rise buildings, could provide a new perspective to this problem. However, we are convinced that a future research into these fields has a firm foundation with this research.

Due to the COVID-19 outbreak in the Netherlands, several adjustments to the procedure have been made. The last interview and the focus group discussion were held online as a result of this. One of the participants in the focus group discussion encountered internet problems. We think this did not affect the outcomes of our research, and might prove to be a more efficient way of working going forward.

Lastly, the lack of a ground truth prevented us to confirm the outcome with reality and make any statements about over- or underestimation. The data we gathered could be compared to a dataset with historical data, once it becomes available, to assess the estimation. If necessary, adjustments can be made to account for these errors.

LIST OF REFERENCES

Actueel Hoogtebestand Nederland. (n.d.-a). AHN Kwaliteitsbeschrivijving. Retrieved March 25, 2020, from https://www.ahn.nl/kwaliteitsbeschrijving

Actueel Hoogtebestand Nederland. (n.d.-b). Process. Retrieved April 1, 2020, from https://www.ahn.nl/process

Ahmad Fuad, N., Yusoff, A. R., Ismail, Z., & Majid, Z. (2018). Comparing the performance of point cloud registration methods for landslide monitoring using mobile laser scanning data. *International Archives of the Photogrammetry, Remote Sensing and Spatial Information Sciences*, *42*(4/W9), 11–21. https://doi.org/10.5194/isprs-archives-XLII-4-W9-11-2018

Alam, N., Coors, V., & Zlatanova, S. (2013). Detecting Shadow for Direct Radiation Using CityGML Models for Photovoltaic Potentiality Analysis . In C. Ellul, S. Zlatanova, M. Rumor, & R. Laurini (Eds.), *UDMS Annual* (pp. 191–210). London, United Kingdom: Taylor & Francis Group. https://doi.org/10.1201/b14914-23

Altuntas, C. (2015). Integration of point clouds originated from laser scanner and photogrammetric images for visualization of complex details of historical buildings. *International Archives of the Photogrammetry, Remote Sensing and Spatial Information Sciences*, *XL/W4*(February), 25–27. https://doi.org/10.5194/isprsarchives-XL-5-W4-431-2015

Angulo, A., Vega-Fernández, J. A., Aguilar-Lobo, L. M., Natraj, S., & Ochoa-Ruiz, G. (2019). Road Damage Detection Acquisition System Based on Deep Neural Networks for Physical Asset Management. In L. Martínez-Villaseñor, I. Batyrshin, & A. Marín-Hernández (Eds.), *Advances in Soft Computing. MICAI* (Lecture No, pp. 3–14). Springer, Cham. https://doi.org/10.1007/978-3-030-33749-0_1

Beeldmateriaal Nederland. (n.d.). Beeldmateriaal producten. Retrieved March 25, 2020, from https://www.beeldmateriaal.nl/het-verhaal-van-beeldmateriaal

Besl, P. J., & Mckay, N. D. (1992). A Method for Registration of 3D shapes. *IEEE Transactions on Pattern Analysis and Machine Inteligence*, *14*, 239–256. https://doi.org/0162-8828/92

Biber, P., & Wolfgang, S. (2003). The Normal Distributions Transform: A New Approach To Laser Scan Matching. In *IEEE/RSJ International Conference on Intelligent Robots and Systems (IROS)* (pp. 2743–2748). Las Vegas, NV. Retrieved from http://citeseerx.ist.psu.edu/viewdoc/download?doi=10.1.1.10.7059&rep=rep1&type=pdf

Biljecki, F., Heuvelink, G. B. M., Ledoux, H., & Stoter, J. (2015a). Propagation of positional error in 3D GIS : estimation of the solar irradiation of building roofs. *International Journal of Geographical Information Science*.

Biljecki, F., Heuvelink, G. B. M., Ledoux, H., & Stoter, J. (2015b). Propagation of positional error in 3D GIS: estimation of the solar irradiation of building roofs. *International Journal of Geographical Information Science*, *29*(12), 2269–2294. https://doi.org/10.1080/13658816.2015.1073292

Biljecki, F., Heuvelink, G. B. M., Ledoux, H., & Stoter, J. (2018). The effect of acquisition error and level of detail on the accuracy of spatial analyses. *Cartography and Geographic Information Science*, *45*(2), 156–176. https://doi.org/10.1080/15230406.2017.1279986

Biljecki, F., Ledoux, H., & Stoter, J. (2016). Generation of multi-LOD 3D city models in CityGML with the procedural modelling engine Random3DCity. *ISPRS Annals of the Photogrammetry, Remote Sensing and Spatial Information Sciences*, *IV*(September), 7–9. https://doi.org/10.5194/isprs-annals-IV-4-W1-51-2016

Biljecki, F., Ledoux, H., & Stoter, J. (2017). Does a finer level of detail of a 3D city model bring an improvement for estimating shadows? *Advances in 3D Geoinformation*, 31–47. https://doi.org/10.1007/978-3-319-25691-7_2

Biljecki, F., Stoter, J., Ledoux, H., Zlatanova, S., & Çöltekin, A. (2015). Applications of 3D city models: State of the art review. *ISPRS International Journal of Geo-Information*, *4*(4), 2842–2889. https://doi.org/10.3390/ijgi4042842

Bódis, K., Kougias, I., Jäger-Waldau, A., Taylor, N., & Szabó, S. (2019). A high-resolution geospatial assessment of the rooftop solar photovoltaic potential in the European Union. *Renewable and Sustainable Energy Reviews*, *114*(April), 109309. https://doi.org/10.1016/j.rser.2019.109309

Boschman, J. (2017). Niet zomaar zonnepanelen op daken centrum zwolle.pdf. *AD.Nl*, p. 4. Retrieved from https://www.ad.nl/zwolle/niet-zomaar-zonnepanelen-op-daken-centrum-zwolle~a8ae7562/

Broersen, S., vd Berg, N., van Deutekom, C., van Erk, R., Hompes, M., Lijding, K., … Zarbanoui, P. (2018). *State of the State report Solar panels could provide half of Dutch electricity demand*. The Netherlands.

Bryman, A. (2012). *Social Research Methods. Oxford Univesity Press* (4th ed.). New York: Oxford University Press.

Collier, E., Duffy, K., Ganguly, S., Madanguit, G., Kalia, S., Shreekant, G., … Mukhopadhyay, S. (2019). Progressively growing generative adversarial networks for high resolution semantic segmentation of satellite images. *IEEE International Conference on Data Mining Workshops, ICDMW*, *2018*, 763–769. https://doi.org/10.1109/ICDMW.2018.00115

Esri. (n.d.-a). Classify LAS building.pdf. Retrieved April 2, 2020, from https://pro.arcgis.com/en/pro-app/tool-reference/3d-analyst/classify-las-building.htm

Esri. (n.d.-b). Extract Roof Forms for Municipal Development. Retrieved May 26, 2020, from https://learn.arcgis.com/en/projects/extract-roof-forms-for-municipal-development/

Esri. (n.d.-c). LAS Dataset statistics. Retrieved March 30, 2020, from https://pro.arcgis.com/en/pro-app/help/data/las-dataset/work-with-las-dataset-statistics.htm

Esri. (2007). Calculating solar radiation. Retrieved March 25, 2020, from http://webhelp.esri.com/arcgisdesktop/9.2/index.cfm?TopicName=Calculating_solar_radiation

Fischler, M. A., & Bolles, R. C. (1980). Random Sample Consensus: A paradigm for model fitting with applications to image analysis and automated cartography. *SRI International.*

Fouten bij berekening geluid Lelystad. (2017, October 17). *De Telegraf.* Retrieved from https://www.telegraaf.nl/nieuws/825678/fouten-bij-berekening-geluid-lelystad

Freitas, S., Catita, C., Redweik, P., & Brito, M. C. (2015). Modelling solar potential in the urban environment: State-of-the-art review. *Renewable and Sustainable Energy Reviews*, *41*, 915–931. https://doi.org/10.1016/j.rser.2014.08.060

Gelfand, N., Ikemoto, L., Rusinkiewicz, S., & Levoy, M. (2003). Geometrically stable sampling for the ICP algorithm. In *Proceedings of the Fourth International Conference on 3-D Digital Imaging and Modeling, 3DIM* (pp. 260–267). IEEE Computer Society. https://doi.org/10.1109/IM.2003.1240258

Ghodsvali, M. (2018). *3D Modelling of Underground Space for Urban Planning and Management – Providing Basic Planning Insight. Thesis submitted to the Faculty of Geo-Information Science and Earth Observation of the University of Twente for the degree of Master of Science in Geo-Information Science and Earth Observation.* University of Twente. Retrieved from http://adlib.itc.utwente.nl/detail.aspx?parentpriref=

Girardeau-Montaut, D. (n.d.). *CloudCompare: 3D point cloud and mesh processing software*. Retrieved from www.cloudcompare.org/doc

ISO. (2004). ISO/IEC Guide 2:2004, Standardization and related activities - General vocabulary.

ISO. (2013). ISO 19157:2013 - Geographic information - Data quality. Geneva.

Izquierdo, S., Rodrigues, M., & Fueyo, N. (2008). A method for estimating the geographical distribution of the available roof surface area for large-scale photovoltaic energy-potential evaluations. *Solar Energy*, *82*(10), 929–939. https://doi.org/10.1016/j.solener.2008.03.007

Julin, A., Jaalama, K., Virtanen, J.-P., Pouke, M., Ylipulli, J., Vaaja, M., … Hyyppä, H. (2018). Characterizing 3D City Modeling Projects: Towards a Harmonized Interoperable System. *ISPRS International Journal of Geo-Information*, *7*(2), 55. https://doi.org/10.3390/ijgi7020055

Kaartinen, H., Hyyppä, J., Gülch, E., Vosselman, G., Hyyppä, H., Matikainen, L., … Vester, K. (2005). Accuracy of 3D city nodels: EuroSDR comparison. *Proceedings of the ISPRS Workshop Laser Scanning 2005*, 227–232. Retrieved from http://www.isprs.org/proceedings/xxxvi/3-w19/papers/227.pdf

Kausika, B. B., Dolla, O., Folkerts, W., Siebenga, B., Hermans, P., & Sark, W. G. J. H. M. Van. (2015). Bottom-up Analysis of the Solar Photovoltaic Potential for a City in the Netherlands A Working Model for Calculating the Potential using High Resolution LiDAR Data. In *SMARTGREENS 2015 - 4th International Conference on Smart Cities and Green ICT Systems* (pp. 129–135). https://doi.org/10.5220/0005431401290135

Kedzierski, M., & Fryskowska, A. (2015). Methods of laser scanning point clouds integration in precise 3D building modelling. *Measurement: Journal of the International Measurement Confederation*, *74*, 221–232. https://doi.org/10.1016/j.measurement.2015.07.015

Kodde, M. (2016). Dense image matching. *GIM International*, *30*(1), 28–29. Retrieved from https://www.gim-international.com/content/article/dense-image-matching-2?output=pdf

Kumar, K., Ledoux, H., Commandeur, T. J. F., & Stoter, J. E. (2017). Modelling Urban Noise in CityGML ADE: Case of the Netherlands. *ISPRS Annals of the Photogrammetry, Remote Sensing and Spatial Information Sciences*, *IV*(October), 26–27. https://doi.org/https://doi.org/10.5194/isprs-annals-IV-4-W5-73-2017

Kurakula, V. K., & Kuffer, M. (2008). 3D Noise Modeling for Urban Environmental Planning and Management. *Real Corp 008*, *2*(February), 517–523.

Machete, R. F. (2016). *Utilizing 3D GIS Models to Determine Incident Solar Radiation on Buildings*. Tecnico Lisboa.

Mainzer, K., Fath, K., Mckenna, R., Stengel, J., Fichtner, W., & Schultmann, F. (2014). A high-resolution determination of the technical potential for residential-roof-mounted photovoltaic systems in Germany. *Solar Energy*, *105*(February 2019), 715–731. https://doi.org/10.1016/j.solener.2014.04.015

Ministerie van Binnenlandse Zaken en Koninkrijkrelaties. (2018). *Catalogus Basisregistratie Adressen en Gebouwen 2018*. 's-Gravenhage.

Mwangangi, K. K. (2019). *3D building modelling using dense point clouds from UAV 3D building modelling using dense point clouds from UAV*. University of Twente.

Myronenko, A., & Song, X. (2010). Point set registration: Coherent point drifts. *IEEE Transactions on Pattern Analysis and Machine Intelligence*, *32*(12), 2262–2275. https://doi.org/10.1109/TPAMI.2010.46

Nouvel, R., Schulte, C., Eicker, U., Pietruschka, D., & Coors, V. (2013). CITYGML-based 3D city model for energy diagnostics and urban energy policy support. In *13th Conference of the International Building Performance Simulation Association* (pp. 218–225). Chambery, France.

Onyimbi, J. R., Koeva, M., & Flacke, J. (2018). Public participation using 3D web-based city models: Opportunities for e-participation in Kisumu, Kenya. *ISPRS International Journal of Geo-Information*, *7*(454), 1–20. https://doi.org/10.3390/ijgi7120454

Oude Elberink, S., & Vosselman, G. (2011). Quality analysis on 3D building models reconstructed from airborne laser scanning data. *ISPRS Journal of Photogrammetry and Remote Sensing*, *66*(2), 157–165. https://doi.org/10.1016/j.isprsjprs.2010.09.009

Paardekooper, M. (2015). *Economic Feasibility of Solar Panels in Amsterdam Economic Feasibility of Solar Panels in Amsterdam Assessing and validating the potential of roof top solar panels in the city of Amsterdam*. VU University Amsterdam.

Peronato, G;, Bonjour, S., Stoeckli, J., Rey, E., & Andersen, M. (2016). Sensitivity of calculated solar irradiation to the level of detail : insights from the simulation of four sample buildings in urban areas. *International Conference on Passive and Low Energy Architecture*, (Cities, Buildings, People: Towards Regenerative Environments).

Peronato, Giuseppe;, Rey, E., & Andersen, M. (2018). 3D model discretization in assessing urban solar potential: the effect of grid spacing on predicted solar irradiation. In *3D model discretization in assessing urban solar potential: the effect of grid spacing on predicted solar irradiation* (p. 43).

Peters, R., Commandeur, T., Dukai, B., & Stoter, J. (2018). 3D-inputgegevens voor geluidssimulaties gegenereerd uit bestaande landsdekkende datasets. *Geo-Info*, *6*, 8–12.

Prieto, I., Izkara, J. L., & Usobiaga, E. (2019). The application of lidar data for the solar potential analysis based on urban 3D model, 5. https://doi.org/10.1117/12.2531938

Ronnholm, P. (2011). Registration quality - towards integration of laser scanning and photogrammetry. *Official Publication - EuroSDR*, (59), 6–43.

Rottensteiner, F., Sohn, G., Gerke, M., Wegner, J. D., Breitkopf, U., & Jung, J. (2014). Results of the ISPRS benchmark on urban object detection and 3D building reconstruction. *ISPRS Journal of Photogrammetry and Remote Sensing*. https://doi.org/10.1016/j.isprsjprs.2013.10.004

Schnabel, R., Wahl, R., & Klein, R. (2007). Efficient RANSAC for point-cloud shape detection. *Computer Graphics Forum*, *26*(2), 214–226. https://doi.org/10.1111/j.1467-8659.2007.01016.x

Sirmacek, B., & Lindenbergh, R. (2014). Accuracy assessment of building point clouds automatically generated from iphone images. *International Archives of the Photogrammetry, Remote Sensing and Spatial Information Sciences - ISPRS Archives*, *40*(5), 547–552. https://doi.org/10.5194/isprsarchives-XL-5-547-2014

Stein, A., & Tolpekin, V. A. (Eds.). (2013). *The Core of GI Science: A System Based Approach* (Vol. 2013). Faculty of Geo-Information Science and Earth Observation (ITC), University Twente.

The American Society for Photogrammetry & Remote Sensing. (2011). *LAS version 1.4 - R6. ASPRS, The American Society for Photogrammetry & Remote Sensing*. Maryland. Retrieved from

http://www.asprs.org/a/society/committees/lidar/LAS_1-4_R6.pdf
Toppen, T. . (2016). *The use of 3D city models in real estate valuation and transactions*. Eindhoven University of Technology.
van de Bor, J. (2019, February 21). Luchthavenbesluit Lelystad bomvol fouten. *Een Vandaag*. Retrieved from https://eenvandaag.avrotros.nl/item/luchthavenbesluit-bomvol-fouten/
van Sark, W. (2014). *Opbrengst van zonnestroomsystemen in Nederland*.
Vosselman, G. (2012). Automated planimetric quality control in high accuracy airborne laser scanning surveys. *ISPRS Journal of Photogrammetry and Remote Sensing*, *74*, 90–100. https://doi.org/10.1016/j.isprsjprs.2012.09.002
Vosselman, G., & Dijkman, S. (2001). 3D building model reconstruction from point clouds and ground plans. *International Archives of the Photogrammetry, Remote Sensing*, *XXXIV-3/W4*, 22–24.
Wilson, C. (2014). *Interview Techniques for UX Practitioners: A User-Centered Design Method*. Morgan Kaufmann. https://doi.org/10.1016/B978-0-12-410393-1.00007-7
Wilson, J. P. (2012). Digital terrain modeling. *Geomorphology*, *137*(1), 107–121. https://doi.org/10.1016/j.geomorph.2011.03.012
Wong, K., & Ellul, C. (2012). Enhancing Positioning of Photovoltaic Panels Using 3D Geographic Information. *Proceedings of the 21st GIS Research UK (GISRUK) Conference, Liverpool, UK*. Retrieved from http://www.geos.ed.ac.uk/~gisteac/proceedingsonline/GISRUK2013/gisruk2013_submission_17.pdf
Xiong, B. (2014). *Reconstructing and correcting 3D building models using roof topology graphs*. https://doi.org/10.3990/1.9789036538107
Xiong, B., Oude Elberink, S., & Vosselman, G. (2016). Footprint Map Partitioning Using Airborne Laser Scanning Data. *ISPRS Annals of Photogrammetry, Remote Sensing and Spatial Information Sciences*, *III–3*(July), 241–247. https://doi.org/10.5194/isprsannals-iii-3-241-2016
Zhang, J. (2019). *Developing a comprehensive framework for property valuation using 3D and remote sensing techniques in China*. University of Twente.

APPENDICES

APPENDIX. 1

Questions for the semi-structured interview.

Questions

1. Could you tell me about your work?
2. How is your experience with 3D building models for work?
3. In case you are working with 3D building models, for which applications are you using them?
4. How familiar are you with 3D building models for solar photovoltaic analysis?
5. Who is the user for this application?
6. According to your opinion, what are the most important geodata requirement to reconstruct 3D building models for solar photovoltaic analysis?
7. Which geodata that can be used to reconstruct 3D building models for solar photovoltaic analysis?
8. Who is the data provider? Are the data publicly available?
9. Are you satisfied with the quality of the data that you mentioned for solar photovoltaic analysis?
   a. If yes, explain your answer?
   b. If not, what are the major shortcomings for the data?
10. Think about data integration, in terms of quality and data types or format, do you face challenges in the data that you use?
11. In your opinion, how to deal with the challenge to derive reliable and consistent conclusions?
12. What information and data do you think is needed to derive reliable conclusions for solar photovoltaic analysis?
13. What suggestions from your practice would you provide to improve the 3D geodata for solar photovoltaic analysis?

---

14. (Show demo) From the demo, in terms of completeness, temporal and positional accuracy what quality elements of input data do you think is sufficient to obtain reliable results for assessing the solar photovoltaic potential?
15. For a precise solar potential assessment do you think additional input data is needed?
    a. If yes, could you tell me where such data exists? And who could provide the data?
    b. If no, why?
16. Based on the demo, do you think 3D visualization and analysis is beneficial for your clients/users?
17. If a national standard for 3D input geodata is provided, will it be beneficial for your work?
    a. If yes, what type of information would you recommend to include in this standard?
    b. How do you think it should be delivered and why? (choose): (a) guideline specifications; (b) ready-to-use 3D building model; (c) ready-to-use 3D input data.

APPENDIX 2

Questions for focus group discussion. The questionnaire was presented in Google form.

3D model evaluation

As a part of the last phase of the research we're conducting, we would like to know your perceptions of the model's fitness to the application.

You are invited because you are familiar with this topic. Some of you even involved in the projects of the same topic, some of you even helped me throughout the trajectory of this research. Therefore, I appreciate a lot your presence and feedback on this final stage of my research.

There are no wrong answers but rather different points of view. So feel free to share your thoughts even if it differs from what others have said. We appreciate constructive criticism as well:)

It is compulsory for you to watch the video from this link to see the process of how the 3D building model was generated: https://youtu.be/hDo2g5ti6p4

Fit-for-purpose

This part contains statements regarding the usability of the 3D model, also the model's fitness for the application of solar photovoltaic analysis.

1. Read this statement: For solar photovoltaic potential analysis facade calculation, the 3D model used as an input data and 2.5D model used as an input data for solar photovoltaic potential analysis for rooftop calculation. *Do you agree or disagree with that statement? Please provide your explanation next to your answer.*
2. This part contains statements regarding usability and fitness of the 3D model for the solar photovoltaic potential analysis.
   a. The presented 3D model created for this research effectively provides the required information for solar photovoltaic potential analysis.

Strongly agree	Agree	Neither agree nor disagree	Disagree	Strongly disagree	No response
O	O	O	O	O	O

   b. The presented level of detail of the 3D model is sufficient for solar photovoltaic potential analysis.

Strongly agree	Agree	Neither agree nor disagree	Disagree	Strongly disagree	No response
O	O	O	O	O	O

General validation statements

This part contains statements regarding the usability and further possibilities of the 3D model.

1. The presented 3D model can be adapted for other applications? (Yes/No) *Please specify the application.*
2. Please list and explain what according to you can be further modified and improved?

Strongly agree	Agree	Neither agree nor disagree	Disagree	Strongly disagree	No response
O	O	O	O	O	O

3. Please list and explain the major benefits you think the presented 3D model has?

Strongly agree	Agree	Neither agree nor disagree	Disagree	Strongly disagree	No response
O	O	O	O	O	O

Data Integration

This part contains statements regarding usability and effectiveness regarding the integration of point clouds. If you need further elaboration for your answer, please fill "Other".

Point cloud integration is the main process in this research besides the 3D building model generation. The objective of this process is to compensate for each drawback point cloud datasets. Moreover, to obtain a point cloud dataset with higher quality determined by higher density, improve the temporal quality and maintain the spatial accuracy.

In this research, we used point cloud obtain from LiDAR and DIM. To process this point cloud dataset as a pre-processing phase, the data quality elements from ISO 19517:2013 (ISO, 2013) were used. Three out of six elements were applied. The techniques applied for pre-processing were derived from these three elements as well. Those are completeness, temporal quality and positional accuracy.

Derived from the explanations of completeness from (ISO, 2013), completeness can be measured by "is there any unmatched data?" or "how complete the point clouds compare with the ground truth?". Therefore, for this element visual inspection by comparing two datasets was done as a first screening. Afterwards, the point density calculation was done to determine the quality of the point cloud and classification process to classify the building as the main interest. To integrate both point clouds we used relative positioning algorithm, Iterative Closest Point (Besl & Mckay (1992)).

1. The presented method regarding integrating point cloud obtained from LiDAR and DIM is useful in another application. (Yes/No) *Please specify the application.*
2. Integrating point cloud, obtained from LiDAR and DIM, appears to improve data completeness.

Strongly agree	Agree	Neither agree nor disagree	Disagree	Strongly disagree	No response	Other
○	○	○	○	○	○	○

3. Integrating point cloud, obtained from LiDAR and DIM, appears to improve data actuality/temporal quality.

Strongly agree	Agree	Neither agree nor disagree	Disagree	Strongly disagree	No response	Other
○	○	○	○	○	○	○

4. Integrating point cloud, obtained from LiDAR and DIM, appears to improve the spatial accuracy.

Strongly agree	Agree	Neither agree nor disagree	Disagree	Strongly disagree	No response	Other
○	○	○	○	○	○	○

Comparison between DSM

Legend

Value

20,2914

3,208

Spatial Reference
Name: RD New

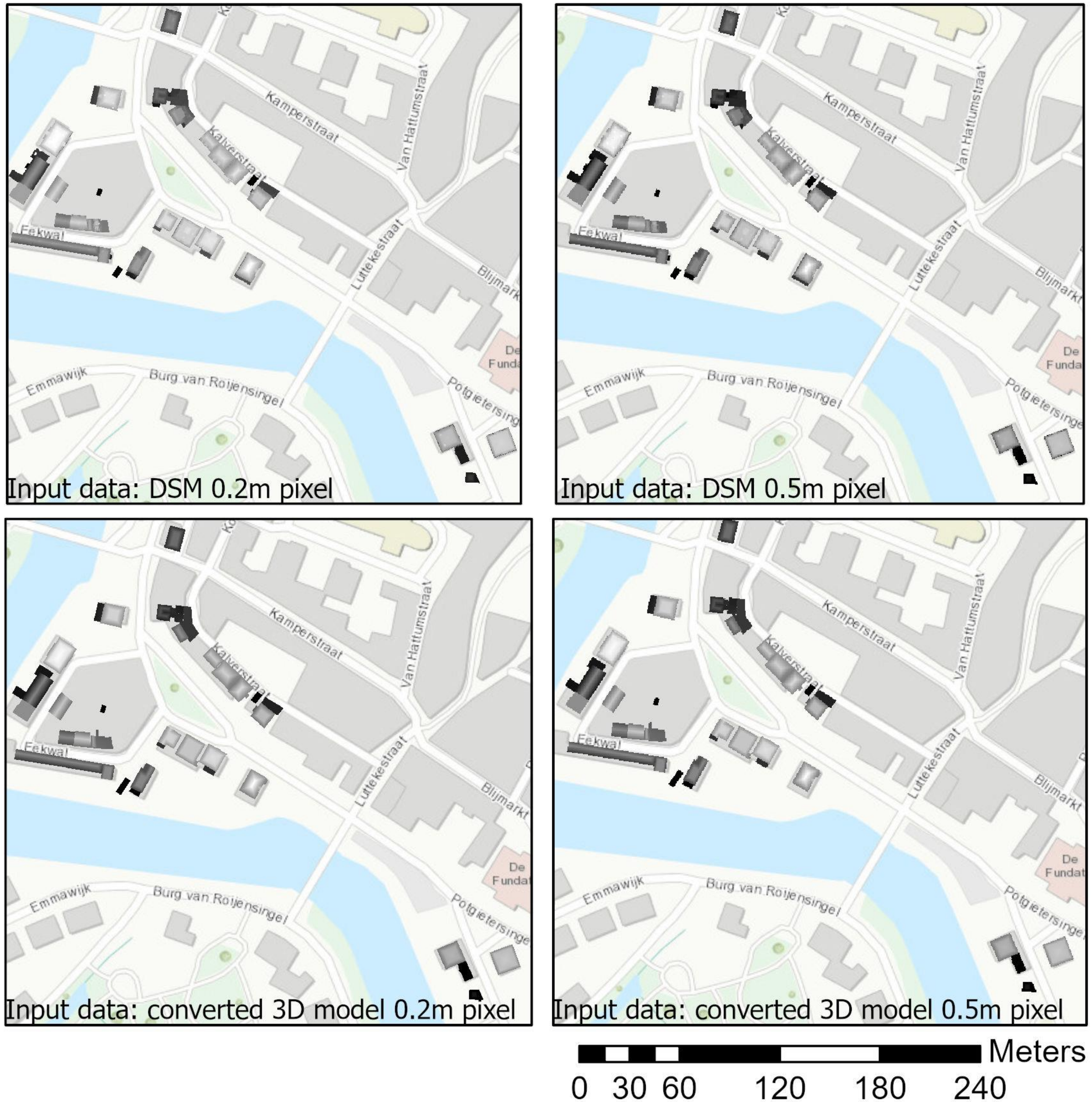

Comparison result of solar radiation calculation

Legend

Solar radiation

kWh/m2

1033,34

26,7421

Spatial Reference
Name: RD New

Comparison result of roof slope calculation

Legend

Building footprint

Roof slope (degrees)

- ≤1,72
- ≤3,43
- ≤5,71
- ≤8,53
- ≤11,3
- ≤14,04
- ≤16,7
- ≤21,8
- ≤30,96
- ≤45
- ≤90

Spatial Reference
Name: RD New

Comparison result of roof orientation calculation

Legend

Building footprint

Roof orientation

- Flat
- North
- Northeast
- East
- Southeast
- South
- Southwest
- West
- Northwest
- North

Spatial Reference
Name: RD New

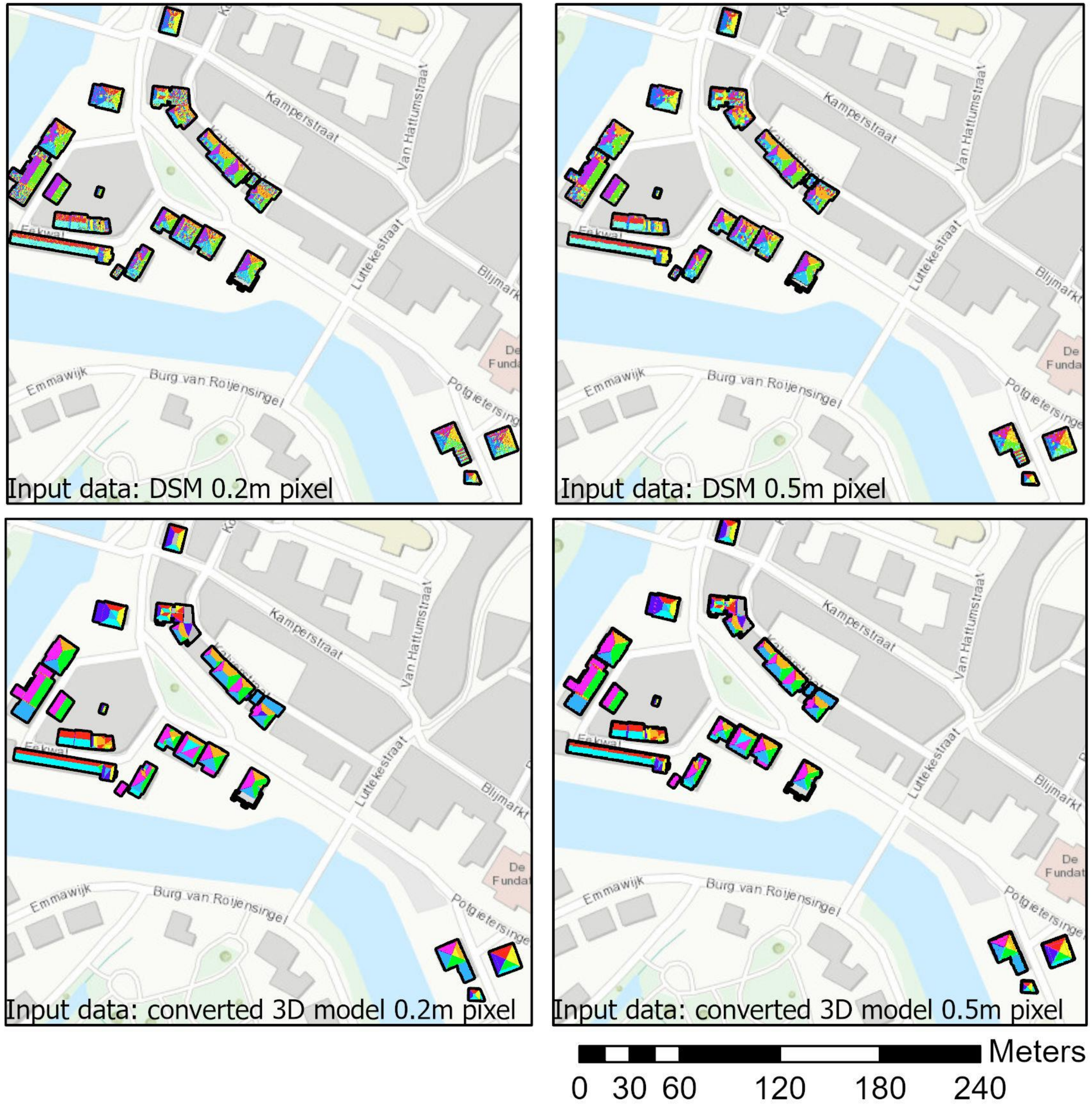

Comparison result of solar photovoltaic potential analysis

Legend

Building footprint

Energy to harvest per building in MWh for year 2019

- ≤4
- ≤14
- ≤27
- ≤60,00
- ≤102,00

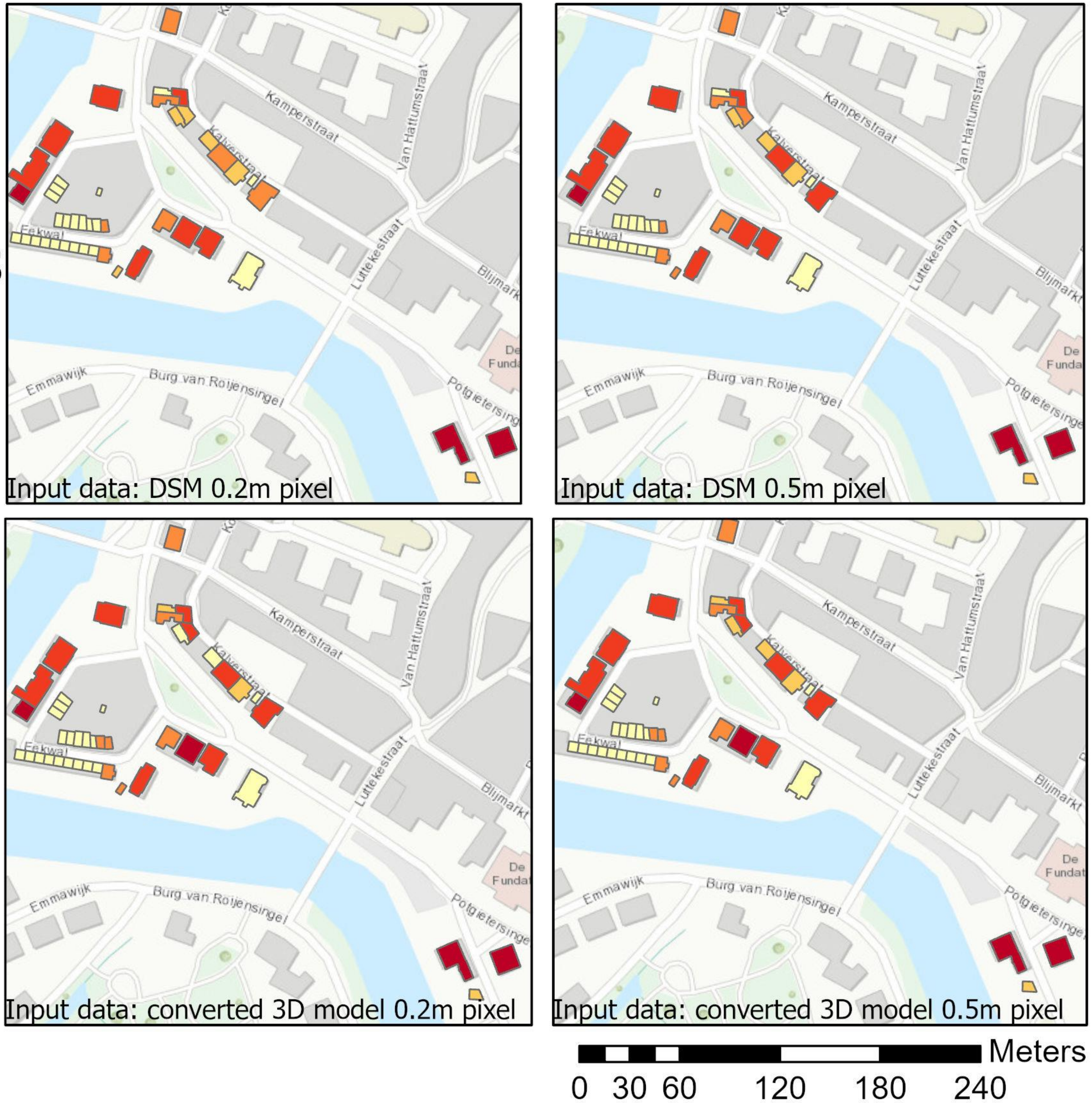

Spatial Reference
Name: RD New